Journal of Manufacturing Processes 101 (2023) 1257–1274

Contents lists available at ScienceDirect

Journal of Manufacturing Processes

journal homepage: www.elsevier.com/locate/manpro

Advances in powder coating of metal components: A case study for wire die springs

Gianluca Rubino [a], Simone Venettacci [b,*]

[a] Università degli Studi della Tuscia, Department of Economics, Engineering, Society and Business Organization, Largo dell'Università, 01100 Viterbo, Italy
[b] University of Rome 'Niccolò Cusano', Department of Engineering, Via Don Carlo Gnocchi 3, 00166 Rome, Italy

ARTICLE INFO

Keywords:
Fluidized bed
Polymer powder
Protective coating
Coverage problem
Complex-geometry components
Scratch test

ABSTRACT

The subject of the present paper deals with the description of an innovative coating process, based on polymer powder fluidized bed technology, applied in combination with an adhesive silicone primer. This study aims to overcome the problems of traditional coating systems for mechanical complex-geometry components, for applications where high precision in thin film deposition and high coating uniformity, at a micrometer level, are required. In this context, the case study of wire die spring coating is here proposed, carrying out a validation of the proposed technical solution, compared to the traditional process based on electrostatic coating, through an aesthetic, morphological and mechanical experimental characterization. The results showed that the innovative deposition system ensures excellent aesthetic performance, depositing a homogeneous coating, with a constant thickness of ~15–20 μm, on the surface of the complex geometry component analyzed, as opposed to ~25–90 μm for the traditional process. The proposed technique also ensures an excellent coating uniformity both inside the coils and on the external surfaces, as well as a complete protective coverage of the springs and their uniform coloring, with significantly lower consumption of coating powder, thus verifying the full technological feasibility of the fluidized bed deposition process, which is applicable also on non-conductive surfaces. Finally, the surface morphology of the specimens coated with the advanced system showed a memory effect of the substrate, while the analysis of the mechanical behavior remarked a higher fragility in terms of scratch test resistance, typical of thin films, compared to the reference.

1. Introduction

The present work studies the problems of traditional systems for the coating of complex-geometry components, in order to provide an innovative, sustainable and easily industrializable solution. The application of surface coatings has both aesthetic-morphological and functional targets, i.e. typically to prevent chemical corrosion [1] and mechanical wear [2], by providing a barrier effect to the metal substrate [3,4]. Current polymer coating methodologies are based on the use of liquid [5] or powder coatings [6,7]; the former are typically applied by spraying systems, which generate a smooth, highly aesthetically pleasing surface, but requiring high skill and precision, not allowing to recovery the overspray, and also entailing the need for hazardous waste disposal and the adoption of expensive and invasive personal protective systems for operators [8,9]. The latter are easier to apply, provide greater coating strength, and can be applied through a wide range of techniques, i.e. fluidized beds (hot dipping or electrostatic ones), flame spray, molding, or electrostatic spraying (either corona gun or triboelectric) [10,11]. The application takes place inside spray booths, with the possibility of recovering the overspray, ensuring a better efficiency of the process, simple and flexible [12,13]; moreover, the application of dry coatings, or not using solvents, ensures a more sustainable and environmentally friendly process, as well as safer for operators [8,14]. The main issue linked to the use of powders is associated with the orange peel effect, or a marked surface waviness, which is responsible for poor surface quality and uniformity of the painted products [12,15]. This phenomenon is mainly attributable to a much higher viscosity of the powder (during the curing phase in the oven), compared to a liquid paint, which therefore makes it difficult to level on the substrate surface.

The original technique for applying powder coatings was based on the use of a fluidized bed (FB) [16], or a large powder container, invested by air currents, within which preheated specimens were immersed, in order to allow the adhesion of the powder, extracted from the container once covered with semi-melted powder, which cross-

* Corresponding author.
E-mail address: simone.venettacci@unicusano.it (S. Venettacci).

https://doi.org/10.1016/j.jmapro.2023.06.067
Received 7 February 2023; Received in revised form 8 April 2023; Accepted 29 June 2023
Available online 12 July 2023

linked in contact with the substrate. This technique is called hot dipping (HD) [17], it allows full coverage of the component, even for complex geometries, and it is still currently used for the deposition of thick coating films, i.e. ~250–800 μm, with a transfer efficiency around 100 % [18,19]. A further issue is related to the low thickness uniformity, with a thickening of material on concave geometries, and a scarcity on convex ones, due to an inability of the paint to accumulate on them [20]. To date, this technology is still preferred for coating processes based on thermoplastic powders, such as polyethylene and nylon, while, for thermosetting powders, systems of an electrostatic nature, i.e. based on the corona effect, are preferred [12,21].

Electrostatic coating is typically applied by electrostatic spray deposition (ESD), i.e. by applying a high-voltage potential to the electrode of a corona gun and grounding the object to be coated, in order to generate a non-uniform electric field between the gun and the substrate, which moves the powders toward the component to coat and allows them to adhere to it, through precisely an electrostatic force [22]. An alternative to spraying systems are electrostatic fluidized beds, which are FB systems in which the adhesion of the fluidized powder to the component is not based on heat, as in hot dipping, but on the application of an electrostatic field [19,23]. The mechanism underlying electrostatic deposition, i.e. corona effect, is mainly limited by two phenomena, which significantly worsen the final aesthetic and functional performance: the first is back-ionization [21], i.e. the generation of an opposite electric field, once the first layer of powder is deposited, resulting in the formation of micro-craters on the surface and an aesthetic performance, as anticipated before, conspicuously to orange peel [12,22]. The second phenomenon is related to the Faraday cage effect [24,25], i.e. in the presence of deep recesses, the material fails to deposit evenly, generating very thick films on the edges of the recesses, while an absence of coverage within them, resulting in an uneven coating with wide thickness variability [15,26]. It represents a strong limitation for complex-geometry, preventing the deposition of a homogeneous, continuous, and low-thickness film with a good coverage [27]. At the industrial level, the solution typically proposed to achieve acceptable pigmentation is based on using a larger amount of powder. However, this approach does not represent a real solution to the problem, since there is always a greater accumulation of powder on the exposed surface of the component to be coated, resulting in a considerable thickness and a strong color shade; while, in the inner areas, thus more hidden, a very thin layer of powder is deposited, with lower mechanical properties, moreover with a decidedly different coloring than in the more exposed areas [21,24]. These effects add up to an increased consumption of coating material, making this powder deposition process certainly inefficient and therefore improvable [28,29]. At the same time, HD technology cannot be considered a viable solution, as it is unable to guarantee thin and uniform covering films. Neither can liquid coating guarantee the deposition of a continuous, homogeneous, low-thickness film on mechanical components [30].

Thus, the current state of technological development of deposition techniques is still insufficient to be able to provide a viable, efficient and sustainable solution for the coating of complex-geometry components, in applications where high precision in thin film deposition and high coating uniformity are required. In this area, the goal of scientific research should be to develop a deposition system that allows rapid deposition of powder coatings, not relying on the corona effect [21,31], thus overcoming the described critical issues, ensuring the same powder transfer capability and better coating quality and uniformity [28,32]. To date, instead, powder coatings research is focused more on the development of innovative formulations, at the level of resins, pigments and fillers [14], in developing low or room temperature curable powder [29], based on laser or UV technologies [28,32], and in functional development, such as antibacterial and deodorizing effect [33], rather than proposing new coating deposition methodologies [34].

Accordingly, the target of the present work is to present an innovative system for the deposition of polymer powder coatings on complex-geometry components, whose application within a fluidized bed is based neither on heat nor on electrostatic fields, but rather on the use of an adhesive primer. The purpose of the proposed process is to overcome the limitations of traditional technologies in order to ensure high coating uniformity, even for very small thicknesses, as required in precision mechanics, allowing deposition even on non-conductive surfaces. In this context, a comparison was made between the properties of wire die springs, i.e. a mechanical component with high complexity geometry, produced with traditional technology, i.e. ESD, and innovative system, i.e. a FB-based powder deposition system, characterizing the coated components in terms of mechanical, morphological and aesthetic performance. The need for the application of a continuous, uniform, and low-thickness film is related to the role of this component in the closure of industrial molds: in case of detachment of high-thickness paint, it would interpose itself between the molds, preventing their complete closure, thus generating high rejection rates and costs associated with molded components.

2. Materials and methods

2.1. Materials

The mechanical components with complex geometry examined in this work are wire die springs, whose image is reported in Fig. 1. Specifically, the sample chosen for the analysis is a heavy load spring, made of high-performance special steel, whose main dimensional and mechanical characteristics are reported in Table 1, according to ISO 10243:2019 standard [35].

The ISO 10243 standard requires that such components must necessarily meet coloration specifications in order to provide information about their mechanical properties in a quick and easily identifiable manner [36,37]. Specifically, specifications on the coloration of such components are reported in Table 2.

According to Table 2, four different polymer coatings, corresponding to different colors and different spring load capacities, uniquely identified through Reichs-Ausschuß für Lieferbedingungen (RAL) classification, were considered in the present experiment. These coatings were produced by Interpon Powder Coatings (51 McIntyre Rd, Sunshine North VIC 3020, Australia) and belong to the 700 series, which is a series

Fig. 1. Image of the uncoated wire die spring.

Table 1
Dimensions and mechanical properties of wire die springs, heavy load series, according to ISO 10243:2019.

Characteristics	Value
Free length (L_0)	44 mm (±1 %)
Rod diameter (D_d)	16 mm (+0.1; +0.7)
Hole diameter (D_H)	32 mm (+0; −0.7)
Rectangular wire section (b × h)	7.1 × 5.4 mm^2
Number of coil spring	5.5
Pitch	~10 mm
Spring constant (R)	324 N/mm (±10 %)
Estimated life in function of normal load	$3{\cdot}10^6$ cycles at 2530 N $\sim 1.5{\cdot}10^6$ cycles at 3170 N $3–5{\cdot}10^5$ cycles at 3480 N $1–2{\cdot}10^5$ cycles at 3800 N

Table 2
Coloring of wire die springs according to ISO 10243:2019.

Load	Color
Light	Green – RAL 6002
Medium	Blue – RAL 5003
Heavy	Red – RAL 3000
Extra heavy	Yellow – RAL 1004

of epoxy-polyester hybrid powder coatings, designed specifically for manual or automatic electrostatic spray system applications. According to the manufacturer's technical data sheet, the curing time of these powders is 10 min for oven baking at a temperature of 190 °C [38]. Furthermore, in order to improve the specimens' coverage, in addition to the lone polymer paint, the metallized variant, i.e. the 700 series polymer paint with added aluminum flakes, was also considered for each coloration, for a total of eight paint powders analyzed. Finally, given the typical low coverage of the yellow and red colors application, also the fluidized bed deposition of a protective bilayer was studied, thus repeating a second time the experimental procedure required for a single layer deposition.

2.2. Manufacturing process

The traditional coating technology for the investigated components, i.e. wire die springs, is based on the electrostatic deposition process [39,40], with the described consequences of an inability to achieve a continuous and homogeneous, low-thickness film on the components, due to the difficulty of coating inside the coils of the springs, due to the Faraday cage effect [21]. Indeed, such electrostatic action makes it difficult to deposit the coating powder in the recesses between coils, or in the presence of areas with deep indentations, resulting in little or no coloration. As anticipated, to date, at the industrial level, increased powder consumption is used so as to ensure acceptable pigmentation and complete protective coverage of the component, with the disadvantage, however, of greatly differing thicknesses in different coating zones and highly inhomogeneous coloration. In particular, there is a greater accumulation of powder on the outer surface of the spring, with a considerable thickness and a strong color shade, while inside the coils a very thin layer of powder is deposited, poorly adhered and with very weak color shade. Thus, the problems related both to the high consumption of coating powder, and to the deposition of thick and uneven films, make the electrostatic powder coating process certainly inefficient for complex-geometry components, pushing the research toward innovative solutions [14,29]. In this area, the aim of the current research was to develop and fine-tune an innovative FB-based powder deposition process, deposited on adhesive substrates.

Specifically, the procedure proposed for the deposition of the polymer coating followed the different steps below:

- The as-received test specimens were washed in an ultrasonic bath of isopropanol in order to remove the grease present on the surface;
- After being dried in an oven, they were immersed for a few seconds inside a silicone primer in order to make adhesive the spring to be painted;
- The specimen was then immediately immersed for a few seconds in a fluidized bed of polymer powders, in bubble regime (up to 15 m^3/h as flow rate), in order to cover the entire surface;
- The last step involved the final stage of cross-linking the specimen coating, which took place inside a convection oven (model P330, Nabertherm GmbH, Lilienthal, Germany).

FB technology has already been described in several papers in the literature [41–43], as an unconventional and a substitute technique for conventional ones, emphasizing its versatility, in terms of the wide range of possible processing, including metal finishing [44,45] of hard and soft components, industrial washing of metallic and non-metallic components [46], coatings [18,20], paint stripping [47], surface [48,49] and waste treatments [50,51]. This technology also provides fast processing times, avoids the use of solvents, dry working, and ensures excellent process repeatability [46,52]. Several works in the literature have already assured its technological feasibility, also verifying its economic and environmental sustainability, compared to traditional technologies [44,46]. The experimental system through which the adhesive rendered specimens are coated has already been described in other literature works [18,53]. Please refer to Fig. 2 for a graphic representation of the experimental set-up for FB deposition.

The fluidized bed used for the experimentation is equipped with a fluidization column with a diameter of 250 mm and a height of 1.2 m. This column is made of PMMA in order to make it transparent and allow

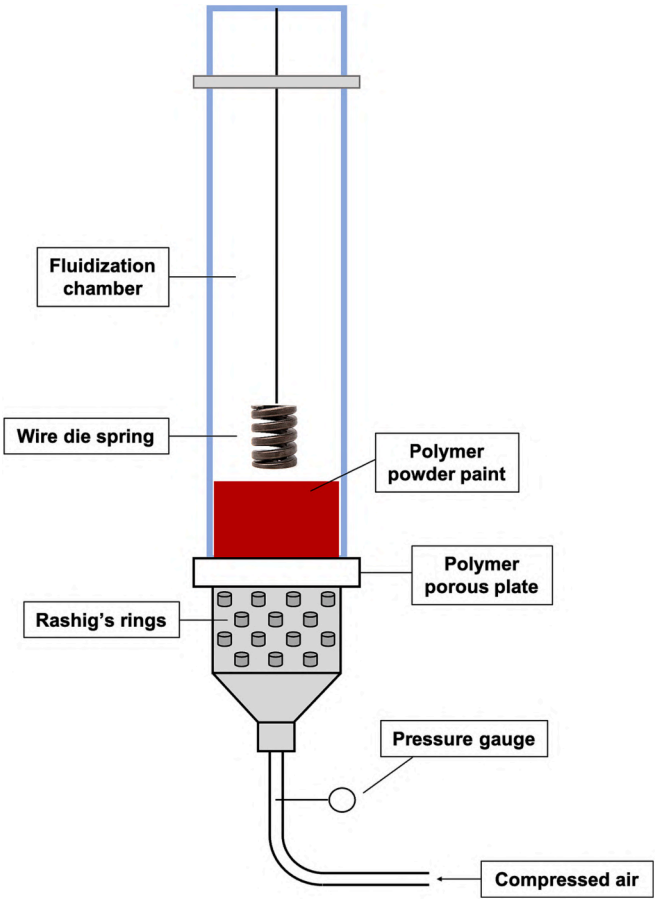

Fig. 2. Experimental setup for FB deposition process.

the fluidization process to be observed from the outside. The walls of the column are 5 mm thick to ensure sufficient stiffness and abrasion resistance. The height of the fixed bed of polymer powder is 200 mm. Below the fluidization column is present the inlet section, also called as homogenization section, filled with porous ceramic material (i.e. Rashig's rings), whose task is to remove the turbulence associated with the incoming air flow and make it uniform. Between the two described columns, there is an air distributor consisting of a 20 mm-thick porous polymer plate, whose presence is necessary to support the weight of the particles in absence of fluidization and at the same time to allow the passage of fluidization air during processing. This component is designed to not alter the velocity distribution produced by the homogenizing section.

2.3. Experimental plan

Table 3 shows the process parameters and levels adopted in the experimental plan for FB-based deposition process. All possible combinations of the factors' levels were considered in the experimental activities.

As clarified in Section 2.1, four colors were considered, as the load to be supported changes, fixed the number of cycles. These scenarios were identified as single layer (SL). In addition to the four types of paints, the corresponding metallic versions were also considered, in order to improve the coverage of the specimens, thus using a total of eight types of coating powders. These scenarios were identified as single layer with metallic filler (SL-M). Following FB deposition, a process of oven curing of the polymer film took place, at a temperature of 190 °C for 10 min of baking, according to the paint manufacturer's technical datasheets, in order to consolidate the coating to the metallic substrate [20,26].

In summary, the total number of innovative experimental scenarios is eight, to which are also added the four reference cases (REF), one for each of the four colors analyzed, in which the specimens were painted according to the state of the art in industrial coatings, i.e. with the same polymer powders, but applied by electrostatic spray, followed by the same cross-linking process at 190 °C for 10 min. In addition to the twelve scenarios considered, the case of the uncoated spring, i.e. the substrate (SUB), was also examined.

As reported in Section 3.1, based on the results of the aesthetic analysis, only for the yellow and red colorations, it was decided at a later stage to coat specimens with a protective bilayer (BIL), in order to solve the problems of low coverage, due to the reduced coating thickness [27], and more closely respect the coloration of the REF specimens. For the deposition of a bilayer protective coating, it was necessary to wait for the single-layer coated specimen to cool, and then proceed again with the steps of the procedure reported in Section 2.2: primer application; fluidized-bed deposition of the powder layer; oven curing.

2.4. Experimental characterization

The experimental specimens were characterized through the succession of aesthetic, morphological and mechanical tests to validate the innovative powder deposition technique, compared to the state of the art in industrial painting. Following the painting procedure, samples were taken from each spring, on which a series of analyses were performed. For this purpose, a metallographic cut-off machine (TR80 Evolution Abrasive Cutter, Remet, Bologna Italy) was used in order to separate the samples from the component to be studied. This high-speed rotating diamond blade cutting machine allows to separate the specimens while limiting the depth of plastic deformation of the material as much as possible.

Table 3
Experimental plan for FB-based deposition process.

Factor		Level	Unit
Color	–	Green, Blue, Red, Yellow	RAL 6002, 5003, 3000, 1004
Metallic filler	Aluminum flakes	M, –	–

Coating thicknesses and their uniformity were evaluated by a digital thickness gauge meter (Megacheck 5F-ST), based on magnetic induction (according to ISO 2178, DIN 50981 - 50982). Coating thicknesses were measured both on the spring heads and bases, performing three measurements on each of the two exposed coils, for a total of six measurements, and on each of the spring coils, performing six acquisitions for each coil, i.e. three on the top surface and three on the bottom one, 120° apart, after sectioning the springs along the longitudinal axis. Coating colors and their uniformity were evaluated by a digital spectrophotometer (BYK-Gardner GmbH, Geretsried, Germany), which operates in the range of visible radiation from 400 to 700 nm, according to multiple international standards (DIN 5033, 5036, 6174; ISO 7724; ASTM D2244, E308, E1164). The surface color measurement is obtained by the identification of three coordinates within a three-dimensional space, in accordance with the international CIELab method [54], based on the principle of spectral reflection:

- L* indicates the luminance. Placed along the vertical axis, it ranges from 0 (black) to 100 (white);
- a* e b* are instead the color components describing red-green and blue-yellow, respectively. The parameter a* ranges from −120 (red) to +120 (green); while b* ranges from −120 (blue) to +120 (yellow).

The color measurements were made at six different points for each of the sample coils, following the same procedure used for measuring thickness. Please refer to Fig. 3 for a scheme of color and thickness measurements, acquired for each spring coil, both on the top and bottom surface.

The coating morphology was analyzed by contact inductive gauge of a CLI profiler (TalySurf CLI 2000, Taylor Hobson, Leicester, UK). In particular, for each sample, square maps of area 4 × 4 mm^2 were acquired by scanning 2000 profiles, with a resolution of 2 μm, along both horizontal directions, to reconstruct the outer surface of the specimens. In addition, 50 profiles, 10 mm long, with a resolution of 1 μm, along the scanning direction, and 2 μm, along the perpendicular, covering an area of 10 × 1 mm^2, were acquired for each sample to calculate the roughness parameters. Then the surface morphology was examined using MountainsMap® 7 software by Digital Surf and the main roughness parameters were processed according to ISO 25178 [55]. The surface morphology was further investigated by acquiring high resolutions images of the coated specimens and their sections, i.e. of the single coils, through a digital camera (Canon EOS 60D, Cernusco sul Naviglio, Milan, Italy). Besides, high-magnification (at 100 and 1000×) micrographs of the coating morphologies were acquired through a Field Emission Gun - Scanning Electron Microscope (FEG-SEM Leo, Supra 35, Carl Zeiss SMT, Inc. Thornwood, New York).

Scratch tests were performed on the coating paints, operating in progressive load mode (Micro-Combi, CSM Instruments, Peseux, Switzerland), using a Rounded Conical Rockwell C diamond indenter, with 200 μm tip radius. The test consists of three different phases: in the first, i.e. pre-scan, the indenter follows and records the surface profile of the sample, for a length of 4 mm, applying an extremely light load of 0.03 N. Back in the starting position, the indenter penetrates the coating at a rate of 1 mm/min, applying a progressive load from 0.03 N to 15 N (in the scan phase); during this phase, both the penetration depth (P_d) and the effective normal load are measured. Finally, in the last phase (i.e. post-scan), the indenter retraces the trace under the action of a very modest load of 0.03 N, measuring the residual penetration (R_d), i.e. following springback. For each sample, the scratch test was replicated three times, on the outer coils of the same spring, performing the tests under controlled conditions, i.e. temperature of 20 °C and relative humidity of 40 %. The residual scratch pattern was rebuilt by the

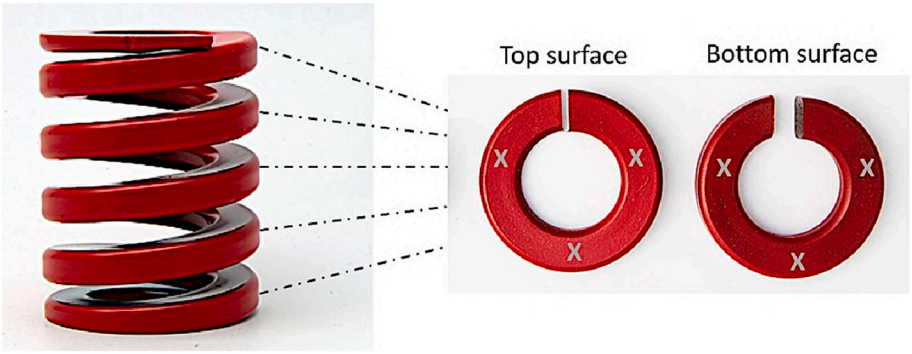

Fig. 3. Scheme of color and thickness measurements, acquired for each spring coil.

profilometer in order to obtain an estimate of the track morphology obtained after the scratch test, specifically by calculating the ditch (V_D) and pile-up (V_P) volumes of the indenter-etched coating zone, by application of the threshold method [56,57], implemented again on MountainsMap processing software. Based on the estimates of these volumes, it was possible to analyze the mechanical behavior of the coating, i.e. the elastic, plastic and brittle contributions of the deformation according to Eqs. (1)–(3), in which V_L represents the volume of the scratch track under load, obtained by reconstructing the volumetric sinking of the indenter into the material, derived by the knowledge both of the penetration depth data and the geometry of the indenter [56,58].

$$Elasticity\ [\%] = 100\frac{V_L - V_D}{V_L} \tag{1}$$

$$Plasticity\ [\%] = 100\frac{V_P}{V_L} \tag{2}$$

$$Fragility\ [\%] = 100\frac{V_D - V_P}{V_L} \tag{3}$$

3. Results and discussion

Fig. 4 reports the SEM micrographs at 100× magnification of the single layer specimens, treated with yellow paint, at varying primer, i.e. P1 or P2, compared with the metal substrate and the reference specimen, i.e. coated by ESD process.

It is worth noting how the choice of primer is decisive, fixed the curing conditions, i.e. 190 °C for 10 min of baking in a convective oven. Specifically, the P1 primer consists of a phenyl-methyl silicone resin, diluted to 25 % within a high boiling point solvent; while the P2 primer, produced using the same silicone resin, is diluted within a lower boiling point solvent, thus more volatile at room temperature. The SEM micrographs reported in Fig. 4 make it clear that the solvent substitution in

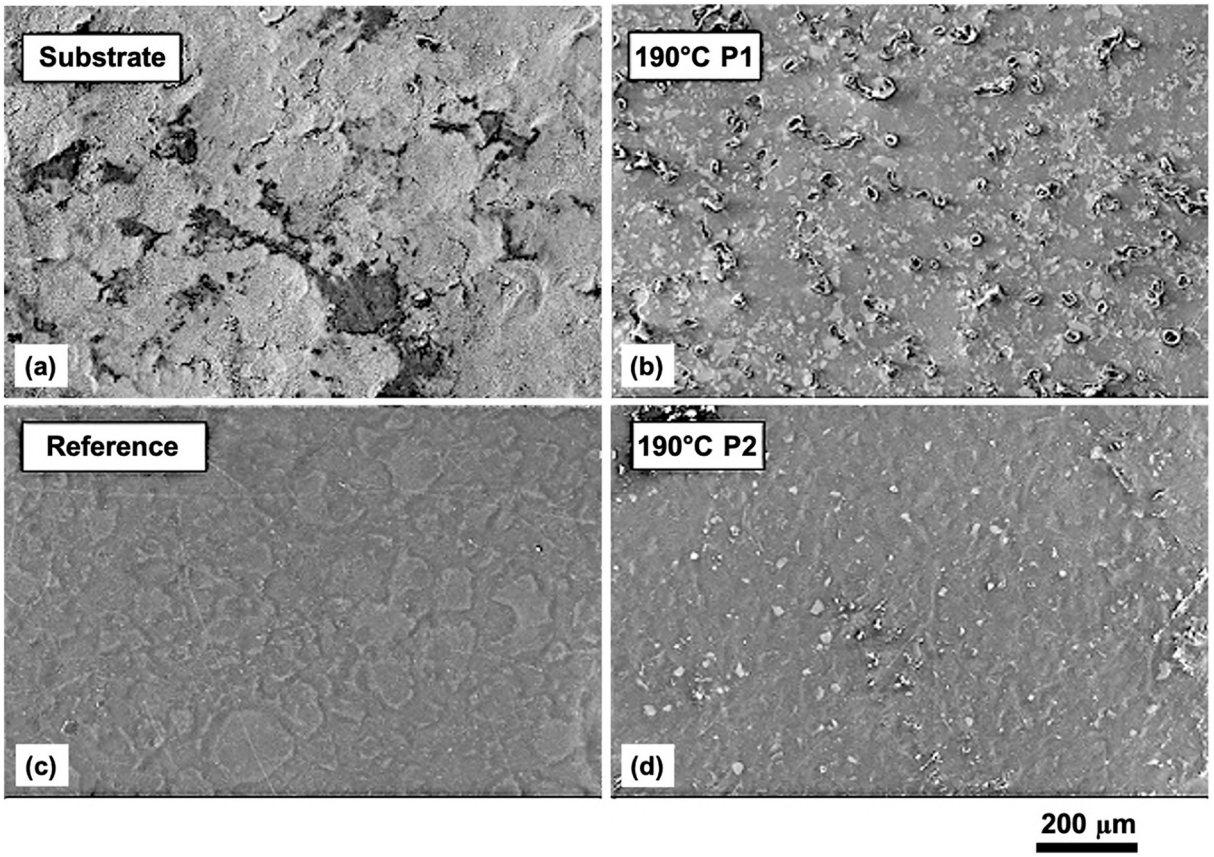

Fig. 4. SEM micrographs of the untreated sample (a) and reference (c), compared with the single layer samples treated with P1 (b) and P2 (d) primers.

the transition from P1 to P2 was crucial in achieving a surface coating much closer to the result obtainable with traditional technology.

The high-magnification (at 1000×) SEM micrographs reported in Fig. 5 show that the P1 primer coating has numerous holes that impair its quality. This defect can be attributed to an outgassing phenomenon that occurs during the cross-linking phase in the oven, due to the high boiling point of the solvent, according to [59]. By switching to deposition with P2 primer, so using a solvent with a lower boiling point, it was possible to avoid the occurrence of this defect, while also managing to save a considerable amount of material, compared to the standard procedure, and to better cover the hidden surfaces of the sample. Considering that the coating has not only aesthetic value, but also a functional one, in terms of protecting the substrate from the corrosive environment, in agreement with [4,23,26,52], the latter aspect cannot be neglected. It is worth pointing out that the same considerations could have been arrived at by observing the surface morphology of specimens coated with other colors, which for brevity of discussion are not reported, since the type of color does not affect the appearance of the surface (from a morphological point of view). Based on these considerations, all test specimens in the experimental plan, coated with the innovative FB-based polymer powder deposition process, were made adhesive by application of P2 primer before the final painting.

In the following sections, i.e. Sections 3.1, 3.2, 3.3, experimental results will be reported with respect to the aesthetic, morphological and mechanical analysis of the heavy load springs, under varying process factors. Out of the need to lighten the discussion, only the color and thickness analysis will be proposed for all RAL in the experimental plan, while the morphological and mechanical analysis will be limited to the case study of the two least covering paints, or yellow and red. It is worth noting that considerations regarding surface topography and mechanical behavior can be extended to the other two colors, or green and blue, which are not reported for brevity of discussion.

Once the technological feasibility of the proposed deposition system on the experimental sample, i.e. heavy load spring, was verified, as reported in the following sections, the FB-based coating process was applied for each color also on the springs with the corresponding effective geometry, i.e. those of the light, medium and extra heavy load series, according to Table 2, thus verifying its technological validity even when the wire cross-section varies, fixed the hole diameter. The positive result of the coating powder deposition for the different examined component geometries is shown in Fig. 6.

3.1. Aesthetic evaluation

The appearance of the experimentally coated wire die springs, applying P2 adhesive primer in all scenarios, was compared with that of the industrially painted springs, according to the standard ESD procedure. The results of color measurement on the base and head of the springs are shown in Fig. 7, while those reported in Fig. 8 are related to the detection of spring coloration on all coils, for all four coating colors.

The polymer film deposited on the base and head of the wire springs shows an excellent overcoating by the electrostatic method, which is associated with lower standard deviations (SD) than the experimental samples, for all three experimental parameters, i.e. for both color deviations (a* and b*) and lightness (L*), for all colorations examined in Fig. 7. The greater external color uniformity achieved by ESD process is mainly related to the deposition of high-thickness coatings, which are significantly greater than for FB specimens (please refer to Fig. 13 of Section 3.2), thus ensuring greater coverage of the substrate. The metallized specimens are characterized by lower SD, especially for yellow coloration (as reported in Fig. 7d), but at the same time they exhibit significantly different color deviations and lightness values than the REF specimens. As a result, there is little resemblance to the reference color of the metallized paint, far less than the non-metallized paint, for each RAL considered. On the other hand, the strength of the proposed innovative technique is related to the uniformity of the coverage, achieved for all the internal coils of the spring, an aspect on which the traditional technology proves to be deficient, according to [24,25,60], for all the proposed colorations, as clearly highlighted from the large SD values shown in Fig. 8. The use of aluminum flakes does not seem to have a positive effect for the green and blue colorations (please refer to Fig. 8a–b), since the SD are still high and the average values deviate even more from the REF values. On the other hand, there seems to be a beneficial effect on yellow coloration (as reported in Fig. 8d), at the level of reducing the SD of the color deviations, but, as with the outer coils, there is a greater difference between the color deviations values and those of the REF. An increase in these variations also occurs for red color (as reported in Fig. 8c), demonstrating poor coloration fidelity of the SLM specimens to the references.

To complete the color analysis, micrographs of internal coils for each of the coated springs, i.e. for each of the studied experimental scenarios, varying in coloration and in presence or absence of metallic fillers, are shown in from Figs. 9 to 12. It is possible to note that the SL coatings provide good coverage and homogeneity, for the green and blue colors, significantly better than the respective references, which instead show low coverage uniformity, with the presence of extensive areas poorly or not at all coated, due to the low internal electrostatically deposited thicknesses, in agreement with [60]. Furthermore, it can be seen that there are no substantial color differences between the coils of the same spring coated through the FB-based deposition process, while the reference suffers from poor uniformity not only on the same coil, but also between the coils of the same spring. The innovative red and yellow

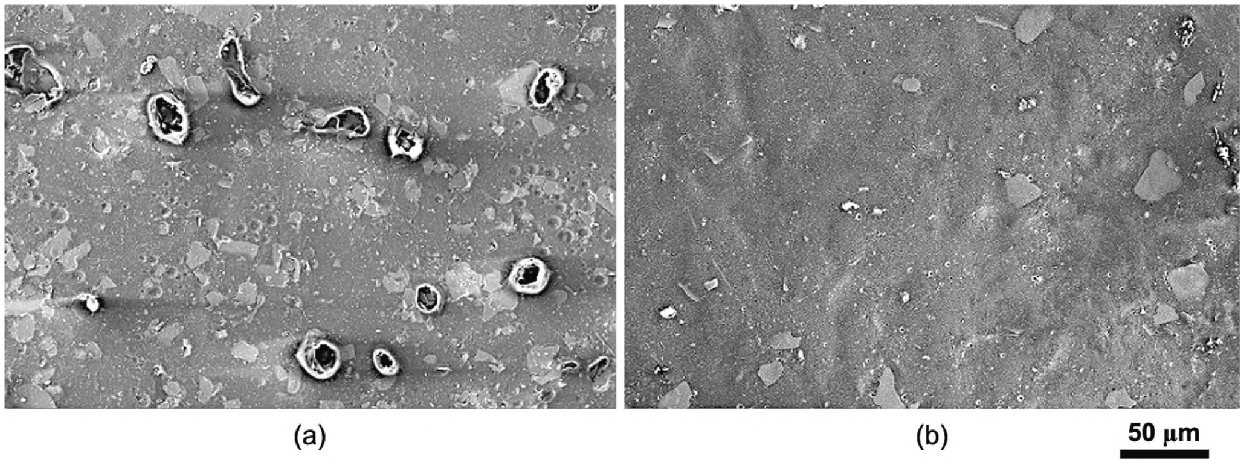

Fig. 5. High magnification SEM micrographs of coated samples, after applying primer P1 (a) and P2 (b).

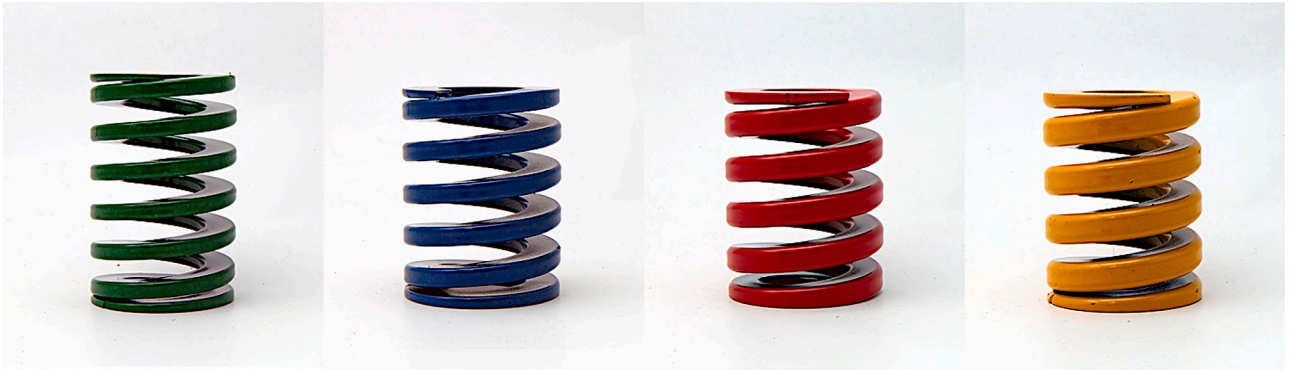

Fig. 6. Coloration of wire die springs by FB-based polymer powder deposition process.

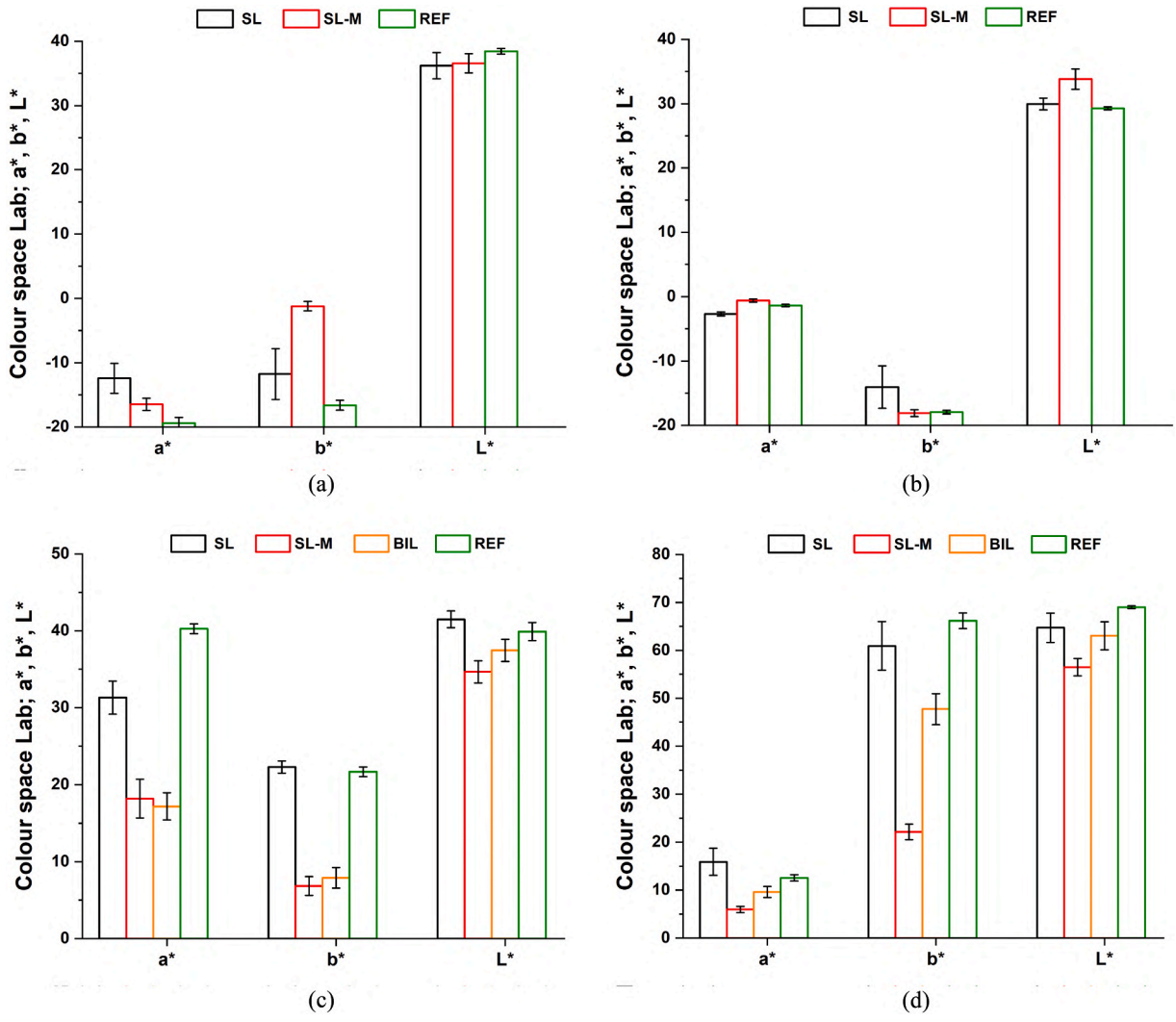

Fig. 7. Color detection on the head and base of the springs, green (a), blue (b), red (c) and yellow (d) painted. (For interpretation of the references to color in this figure legend, the reader is referred to the web version of this article.)

FB coatings (please refer to Figs. 11 and 12), while showing better uniformity than the REF, have low coverage and a visibly different color from the REF. The choice of applying aluminum flakes in the paint seems to positively affect the coverage level for the red color, less so for the yellow; in any case, such metallization produces a noticeable deviation from the REF. In order to improve the coverage of these colors, the application of a bilayer coating was also tested, verifying greater chromatic homogeneity of the surface, i.e. a better degree of covering. The images reported in Figs. 11 and 12 clearly show the greater chromatic homogeneity of the surface. This result is confirmed by the color deviations and lightness for the BIL specimens reported in Fig. 8c–d, which are associated with lower SD and less difference from the REF values.

In summary, the coatings with green and blue colorations showed

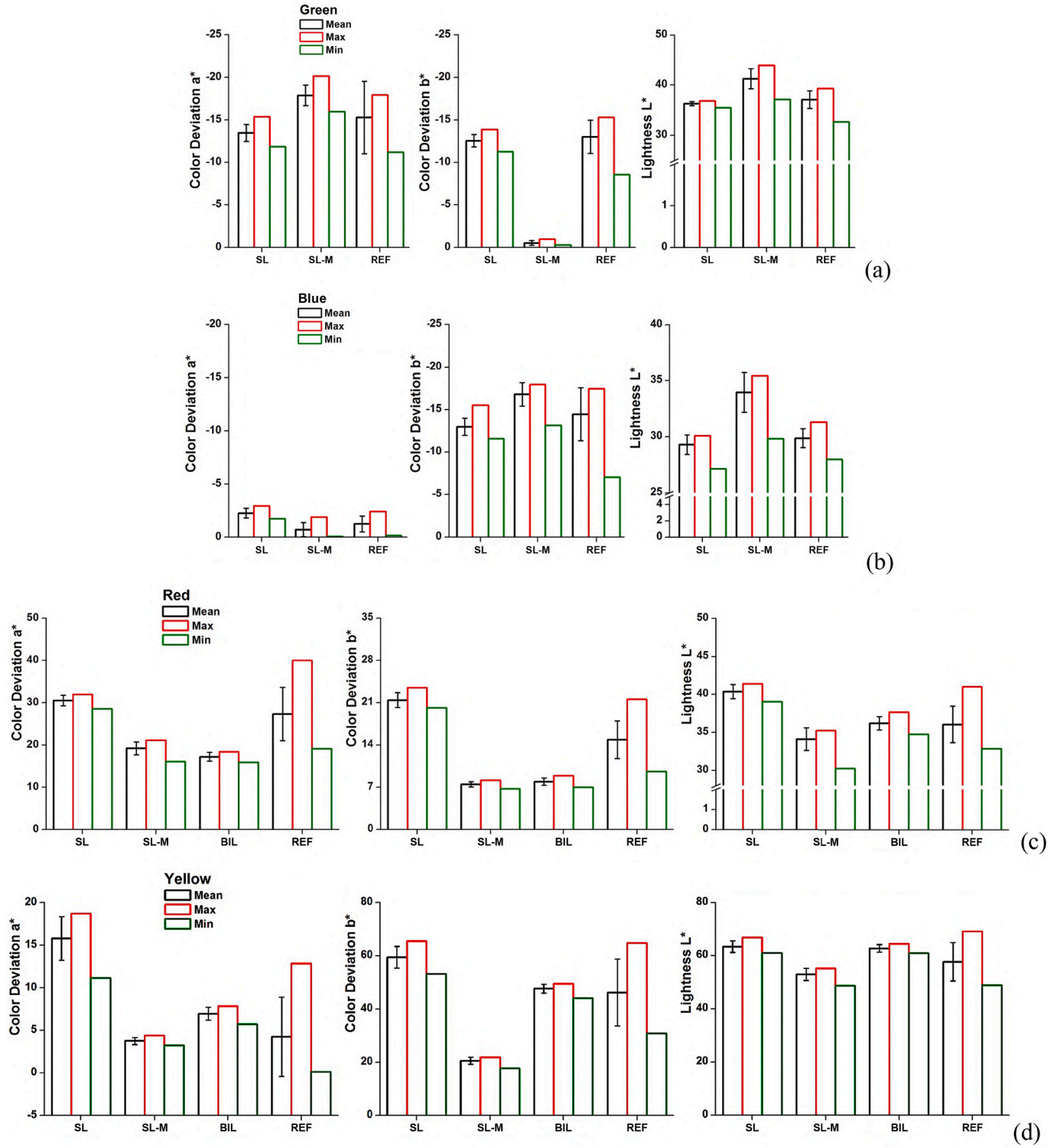

Fig. 8. Color detection on all spring coils, green (a), blue (b), red (c) and yellow (d) painted. (For interpretation of the references to color in this figure legend, the reader is referred to the web version of this article.)

the ability of the FB-based powder deposition process to homogeneously paint the experimental samples. The low coverage associated with the red and yellow colors led to the addition of aluminum flakes in the paint, solving the issue under investigation, but at the same time resulting in excessive color deviation from the REF. The application of a bilayer makes it possible to produce a coating more similar to the reference, solving the coloration problem, especially for the yellow color. The red-colored BIL sample takes on an intermediate aesthetic appearance between the REF and SL-M, resulting in a fairly different coloration from both the SL and REF, as also evident in Fig. 8c.

The next characterization activity involved thickness measurements, both on the head and base of the springs, and on all internal coils, for all proposed colorations. The experimental values are summarized in Fig. 13, in which the results of the internal and external measurements under consideration are compared. The difference in average thickness on the outer surfaces between the coating obtained by the traditional

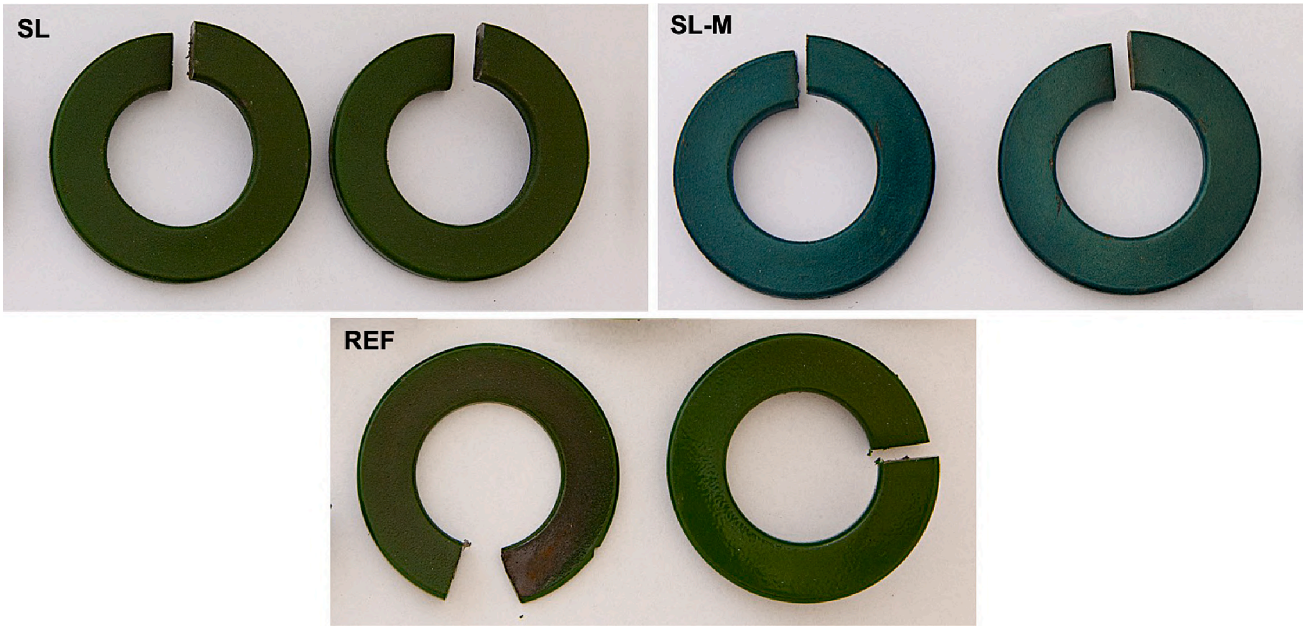

Fig. 9. Micrographs of the inner coils of green-coated springs, under different experimental scenarios analyzed. (For interpretation of the references to color in this figure legend, the reader is referred to the web version of this article.)

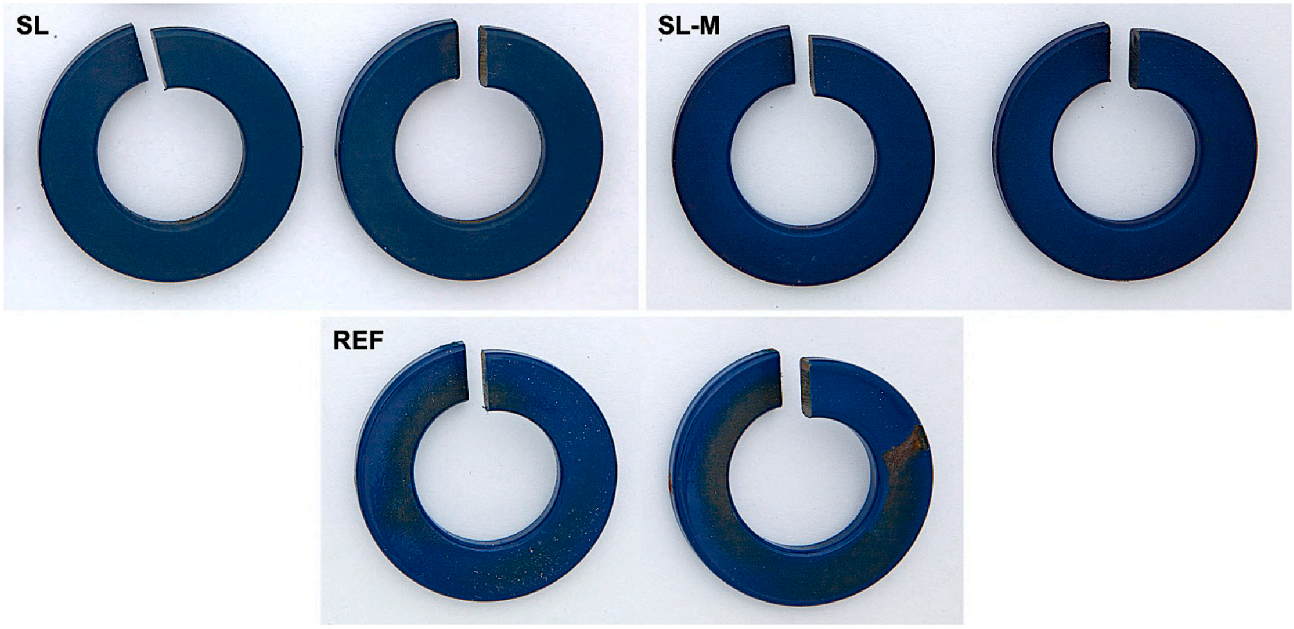

Fig. 10. Micrographs of the inner coils of blue-coated springs, under different experimental scenarios analyzed. (For interpretation of the references to color in this figure legend, the reader is referred to the web version of this article.)

ESD technique, i.e. ~90 μm, for yellow and red color, and i.e. ~75 μm for blue and green, and that obtained by the experimental FB technique, i.e. ~15 μm for green and blue color and ~10 μm for red and yellow color, is clearly shown. It is worth noting that electrostatic deposition on the outer surface is consistent with typical thickness values of powder coatings, ranging from 80 to 120 μm, according to [27]. On the other hand, for the inner surface, an average thickness of ~26–27 μm for the yellow and green colors, ~33 μm for the blue color and ~37 μm for the red color is measured for conventional technology, compared with values of ~16–18 μm for the green and yellow colors, and ~22 μm for the blue and red colors for FB deposition.

The reduction in average thickness is also associated with a very noticeable reduction in SD, which assumes very high values for traditional technology for external coating (i.e. ~8–9 μm for green and yellow, ~18 μm for blue, ~22 μm for red), but even greater inside the spring (i.e. ~18 μm for green, ~22 μm for yellow, ~29 μm for blue, and ~35 μm for red), showing a poor and uneven coverage of the inner coating, with consequent deterioration of surface aesthetic aspect, in agreement with [60]. On the other hand, for FB-based coating, deposited on adhesive substrate, a SD value of ~5 μm is obtained externally, regardless of color, and even lower internally, i.e. ~3 μm, for all colors except blue, for which it settles at ~6 μm, underlining a significantly greater coating uniformity, compared to REF, as already highlighted in from Figs. 9 to 12.

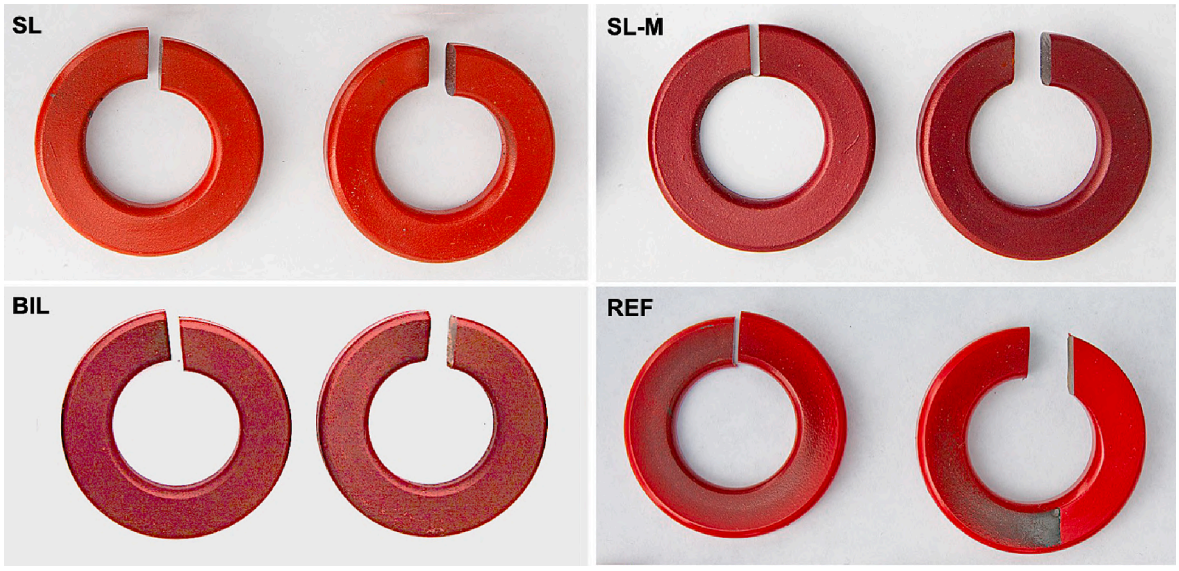

Fig. 11. Micrographs of the inner coils of red-coated springs, under different experimental scenarios analyzed. (For interpretation of the references to color in this figure legend, the reader is referred to the web version of this article.)

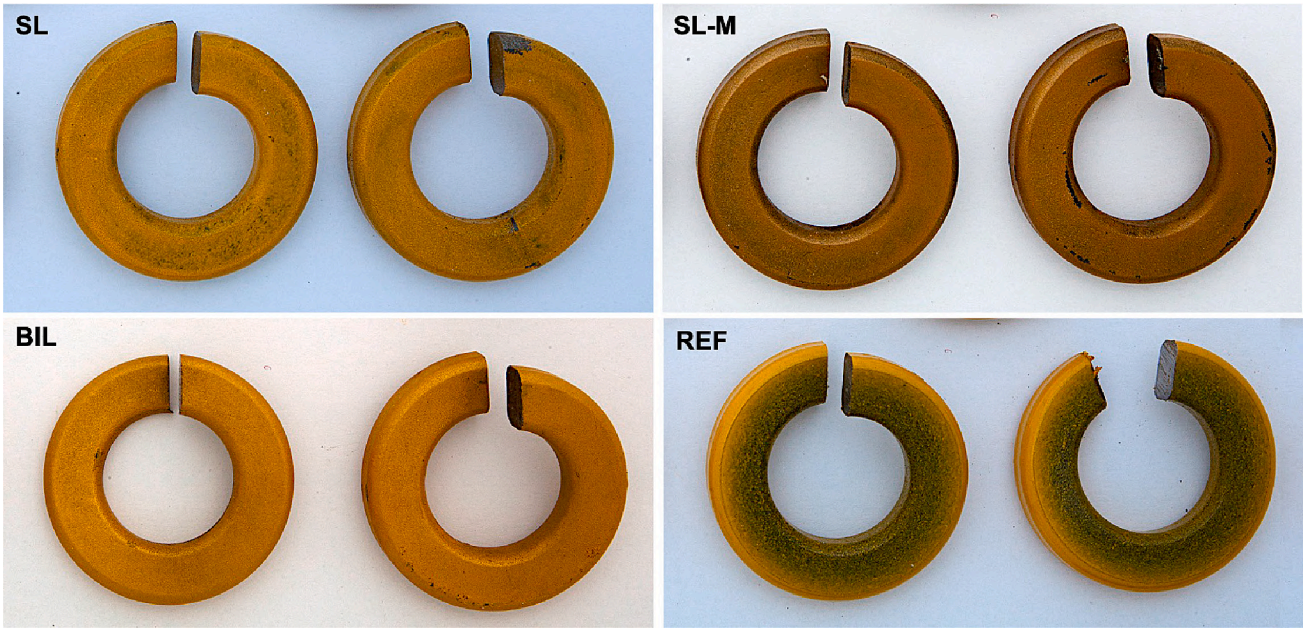

Fig. 12. Micrographs of the inner coils of yellow-coated springs, under different experimental scenarios analyzed. (For interpretation of the references to color in this figure legend, the reader is referred to the web version of this article.)

These results clearly show how, for electrostatic reasons, applying the conventional technology the powder cannot be deposited uniformly over the entire surface of the complex-geometry sample, as the powder cannot effectively penetrate inside the coils, thus coating them unevenly. So, the reference springs will have a very thick coating at the head and the base (i.e. ~75–90 μm, consistent with [27,60]), while a much lesser thickness in the inner coils (i.e. ~25–35 μm for the different colorations), with the presence of uncovered, patchy areas. On the other hand, the experimental system deposits on the substrate a coating of considerably less thickness, i.e. ~15–20 μm, as the color and the presence or absence of metallic fillers vary, with very slight difference between the inner and outer surfaces, demonstrating its ability to coat even parts that are difficult to reach by other coating systems. The considerable reduction of thickness also allows a considerable saving of coating powder, still ensuring a complete covering of the surface. If greater thicknesses were to be deposited, to ensure a more uniform coating for low coverage colors, i.e. red and yellow, the innovative FB-based deposition process would allow it by simply resorting to a bilayer coating, as highlighted in Fig. 13c–d. It is worth noting that there is a consistent growth in thickness, compared to the SL specimens, i.e. ~22–26 μm on the outside and ~33–37 μm on the inside, for the two different colors, but especially a significant reduction in thickness SD, down to ~2 μm, indicating a very high coating uniformity, on each painted surface.

3.2. Morphological analysis

Figs. 14 and 16 show the 3D reconstruction of the outer surfaces of

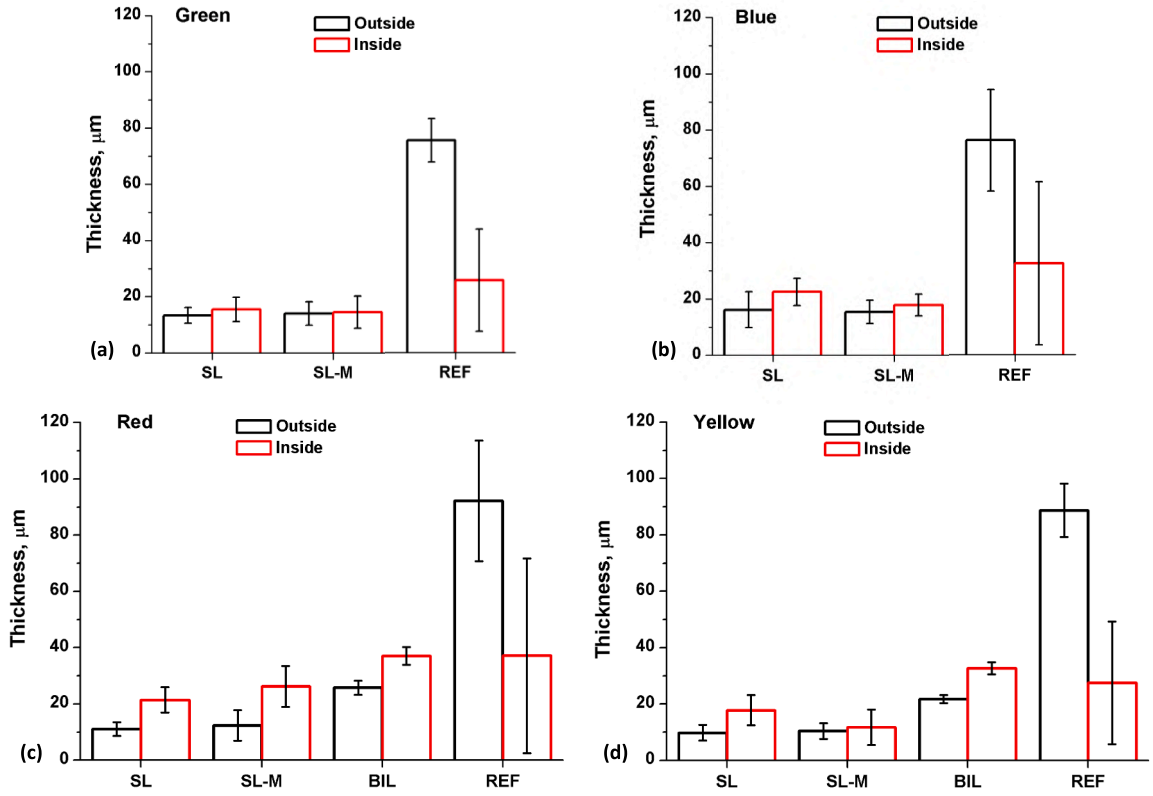

Fig. 13. Measurement of the thickness on the head and the base of the springs (Outside), compared with the values measured on all coils (Inside), for green (a), blue (b), red (c) and yellow (d) painted springs. (For interpretation of the references to color in this figure legend, the reader is referred to the web version of this article.)

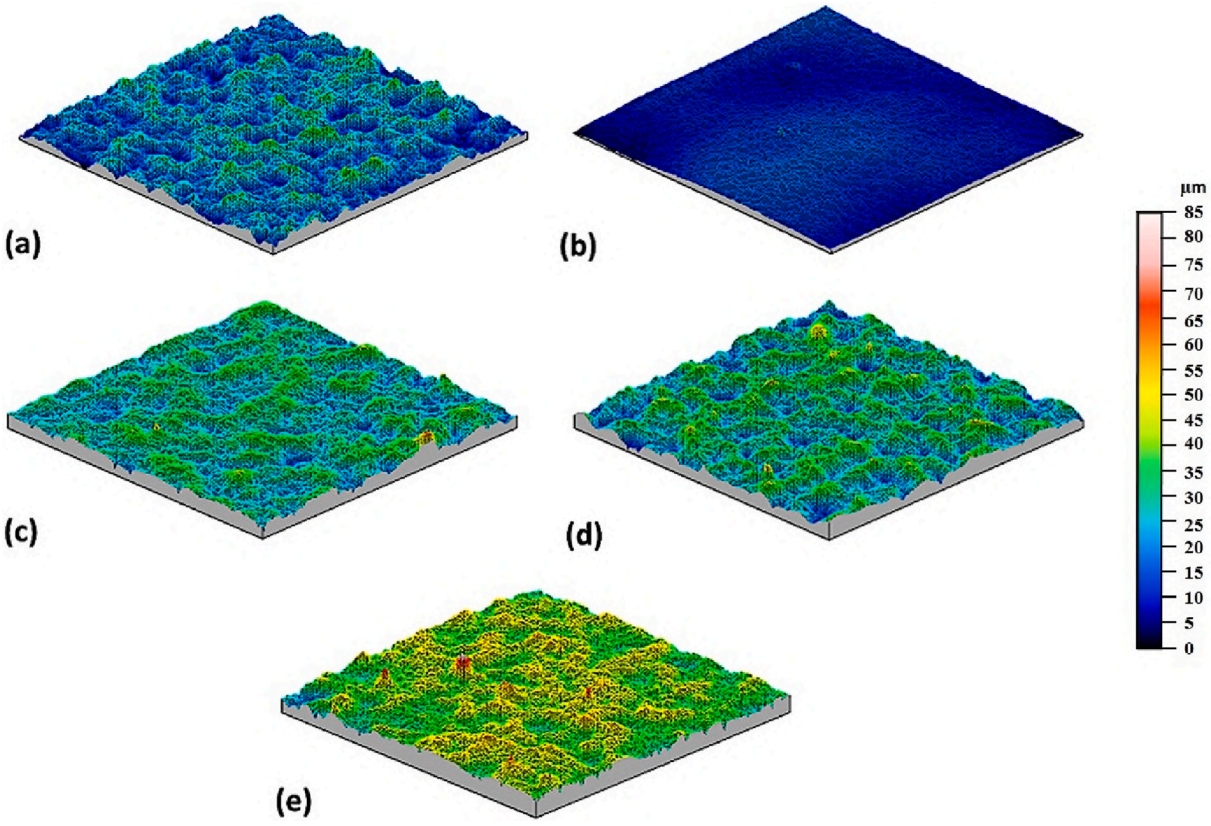

Fig. 14. Surface topography of red-painted springs, as the coating conditions change: (a) SUB; (b) REF; (c) SL; (d) SL-M; (e) BIL. (For interpretation of the references to color in this figure legend, the reader is referred to the web version of this article.)

the springs, by mapping them to the profilometer, for the red and yellow color coating, respectively, for each of the experimental scenarios analyzed. It is worth noting that the traditional coating provides a better surface finish for both colorations, due to the deposition of a thicker polymer coating, which is able to bridge all the peaks and valleys that characterize the surface of the uncoated substrate, according to [18,26,27]. This is different with the innovative FB-based process, as all the specimens in the experiment, independently of the presence of metallic fillers, are characterized by a high roughness, similar to SUB, with slightly less asperity. In fact, applying a powder coating, which maintains a high viscosity during the oven curing phase, its deposition succeeds only partially in smoothing the roughness peaks and filling the valleys present on the surface of the SUB, unlike a liquid one. The BIL specimen, due to the larger amount of deposited material, succeeds in further reducing the roughness peaks, thus showing a superior finishing compared to the SL specimens, though still inferior to the REF. These considerations, which are valid for the yellow and red specimens, can also be extended to the blue and green colorations (not shown for brevity of discussion), indicating how the effect of the coating color of the springs does not seem to affect their surface morphology.

On the other hand, Figs. 15 and 17 show values of surface roughness parameters for red and yellow paint, respectively, for each of the experimental scenarios analyzed. Please refer to Tables A.1 and A.2 in the Appendix for more details. These values confirm what has already been reported following observation of the 3D morphological maps. It can be observed that the FB-coated springs have an average roughness (R_a) of ~1.8–2.1 μm, and maximum roughness (R_z) of ~12.4–14.8 μm, significantly higher than the conventional specimens, by about an order of magnitude, i.e. ~0.23–0.35 μm for R_a and ~2–2.7 μm for R_z, for yellow and red colorations, respectively. It is also worth noting that the roughness values of the fluidized-bed coated springs fairly closely trace the values of the substrate, i.e. ~2.7 μm for R_a and ~14 μm for R_z, due to the deposition of a very thin layer of polymer powder, ~10 μm, less than the R_z of the SUB, which merely follows the underlying profile, with no possibility of filling the valleys and covering the roughness peaks to any great extent, in agreement with [61]. It follows that the springs coated with the traditional method lose trace of the substrate, showing smoothness on contact, in agreement with [26], while the springs painted with the innovative FB-based system retain the corrugation of the base metal, according to a memory effect. The roughness parameters confirm the substantial non-influence of the presence or absence of aluminum flakes, confirming what has already been reported in the discussion about 3D morphological maps. The bilayer deposition treatment allows to reach intermediate roughness values between the single-layer coated samples and traditional ones, in particular for yellow, i.e. ~1.1 μm for R_a and ~6 μm for R_z, confirming how the deposition of a greater coating thickness allows to cover more and thus reduce the surface roughness, mitigating the memory effect characteristic of SL and SL-M specimens. For red, as already observed for coloration, there is a greater difference compared to REF, with roughness values of ~2.2 μm for R_a and ~11.3 μm for R_z. In summary, it was observed that the surface morphology is strictly dependent on the extent of deposited coating thickness, while the other experimental parameters (i.e. color and filler) turn out to be not at all or very insignificant.

3.3. Mechanical behavior analysis

Fig. 18 shows the trend of penetration depth, i.e. the sinking of the indenter into the material under load, and residual depth, i.e. post-scan, as a function of applied normal force, or the scratch track length. As

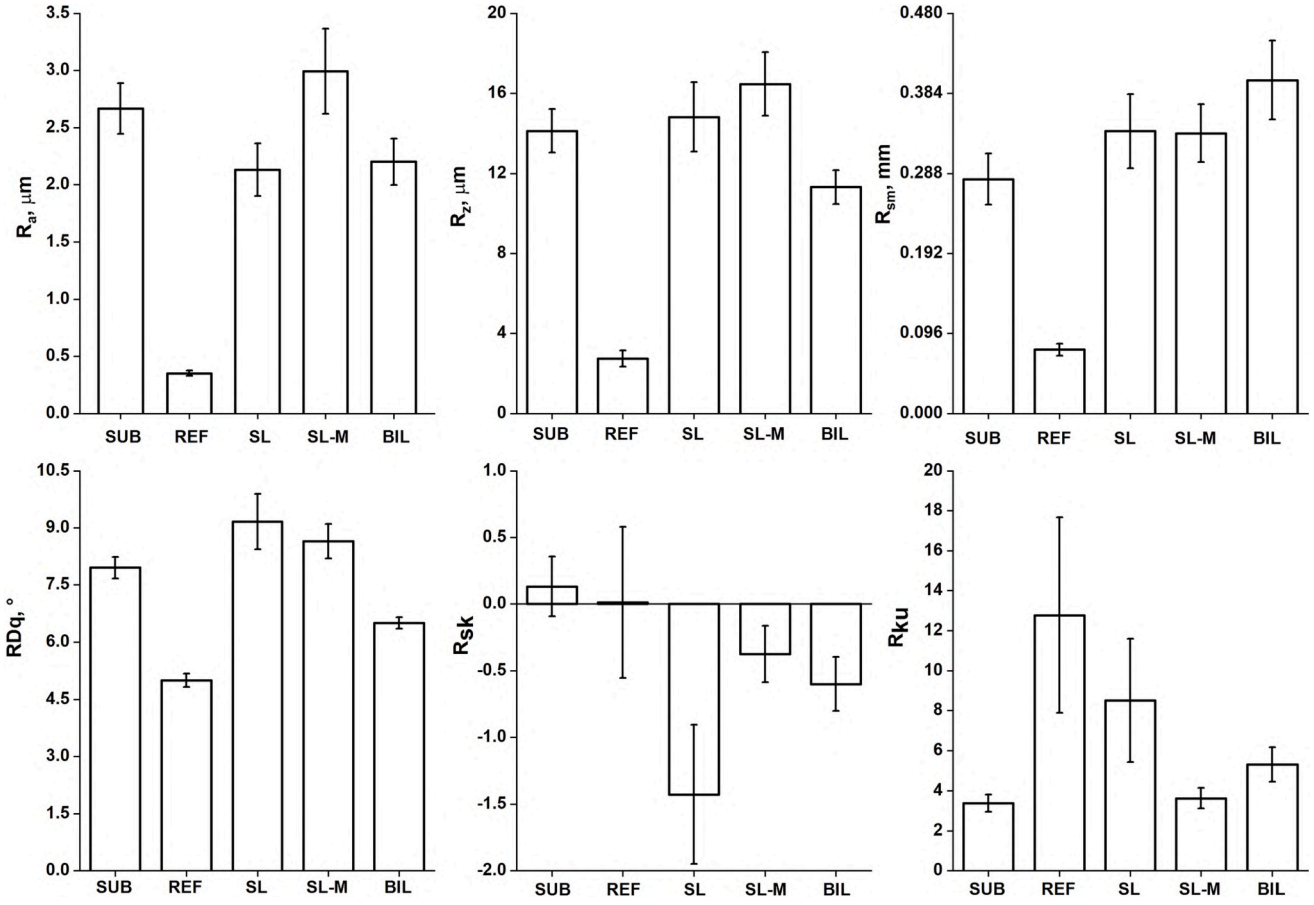

Fig. 15. Roughness analysis of red-coated samples. Please refer to Table A.1 in the Appendix for more details.

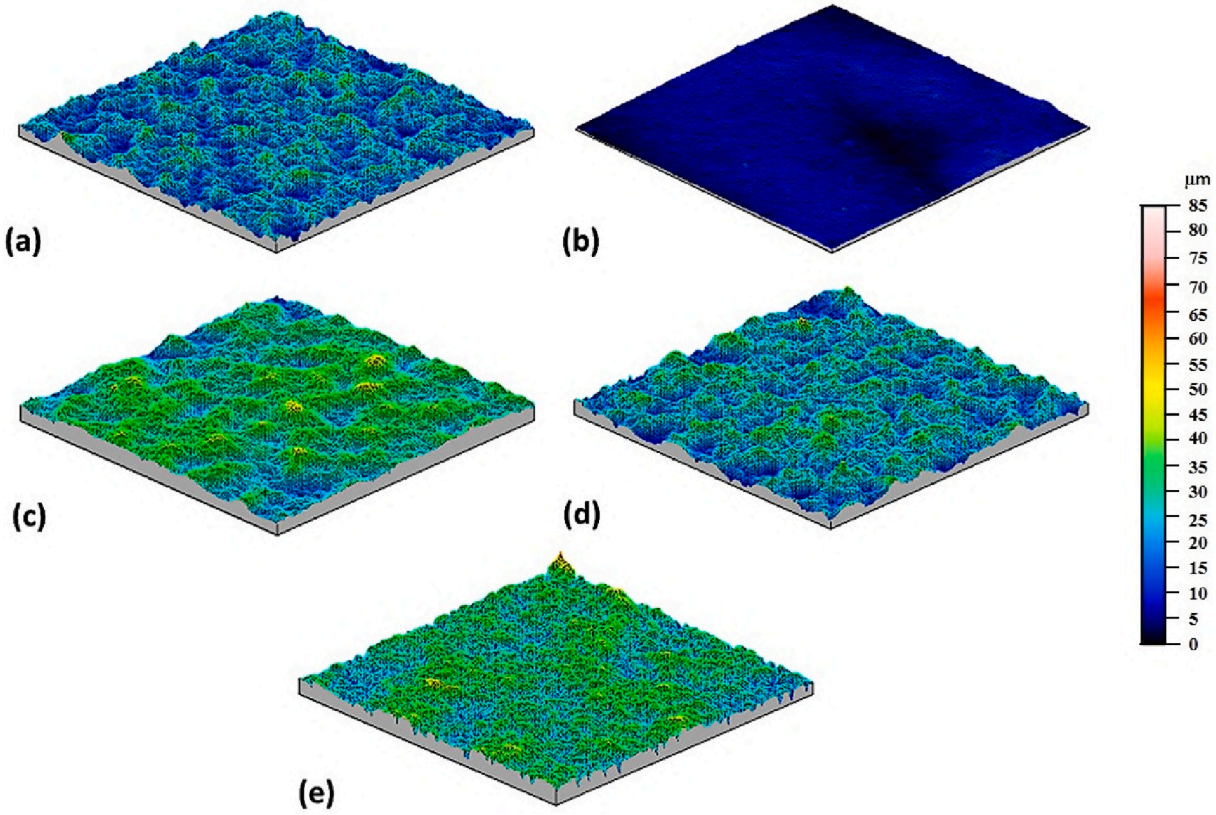

Fig. 16. Surface topography of yellow-painted springs, as the coating conditions change: (a) SUB; (b) REF; (c) SL; (d) SL-M; (e) BIL. (For interpretation of the references to color in this figure legend, the reader is referred to the web version of this article.)

already observed for surface morphology, the mechanical behavior is also not significantly affected by the presence of metal flakes added to the polymer coating. Furthermore, it is observed that in the first part of the P_d curve, there is essentially a similar mechanical behavior between the FB-based coatings and the reference. However, as the load increases, or already for 3–5 N, it can be seen that for single-layer fluidized-bed specimens the P_d settles around a constant value, with a clear reduction in the slope of the curve, indicating that the substrate is reached as a result of material penetration (confirmed by reaching a P_d of ~10–15 µm, in accordance with the coating thickness reported in Fig. 13). The deposition of a thin, high-roughness film thus generates already at low loads such compressive stresses as to compromise the interface with the underlying metal.

On the other hand, for the specimen coated with traditional ESD system, the severity of the test is not such as to reach the underlying substrate, i.e. to stress the spring-coating interface, as evidenced by a continuous increase of the P_d with roughly constant slope, interrupting at ~50 µm (as shown in Fig. 18a–c), thus still far from the extension of the coating thickness, of ~90 µm. The P_d trend of the REF is also much more linear than the FB-coated specimens, as the REF is significantly smoother. As for the SUB, the indenter penetrates little into the material, due to a significantly higher stiffness.

The R_d graphs of REF specimens, reported in Fig. 18b–d, show an increasing trend with loading force, followed by sharp and conspicuous decrease in the last section of the trace, due to the springback of the material. On the other hand, this behavior is little noticeable for the SL specimens, since a detachment of the coating, for its entire thickness, has occurred. The BIL specimens, despite a higher thickness than the SL, i.e. ~25 µm, do not show substantial differences from other types of FB-based specimens in terms of scratch resistance, at the level of penetration and residual depths.

To better characterize the mechanical behavior of the components painted with innovative and traditional techniques, the volumes of the ditch (V_D), of the pile-up (V_P) and of the track under load (V_L) were estimated. The results, for the two examined colors, i.e. red and yellow, are shown in Fig. 19a–b, respectively.

The experimental values of V_D, V_P and V_L show that the ditch and pile-up volumes are significantly higher for the reference specimen. As anticipated, the greater thickness allows for greater penetration of the indenter, as opposed to the experimental specimens, for which already at ~3–5 N of normal load it comes in contact with the substrate, made of special steel and therefore considerably harder to scratch. In Fig. 19a–b, it is worth noting that the V_P is greater than the V_D, for the conventional coating alone: this phenomenon can be explained considering that on the sides of the trace a "swelling" effect of the material is generated, during scanning, on which the ditch material is then deposited, forming high pile-ups. This phenomenon is observed for the REF specimens of all colors analyzed (please note that the blue and green color were not reported for brevity of discussion), but not for the experimental specimens, due to a different thickness, or a different tensional state to which the metal-polymer interface is subjected.

Based on Eqs. (1)–(3), it was possible to characterize even better the mechanical behavior of the coatings, in terms of the elastic, plastic and brittle deformation contributions. These results are reported in Fig. 20 for the red and yellow coatings.

For the traditional coating, a negative value of brittleness is observed, in agreement with the previously stated discussion, or with a value of V_P greater than V_D. On the other hand, for the experimental specimens, coated with an innovative FB-based powder deposition process, applied on adhesive substrates, a more brittle behavior is confirmed, due to the deposition of a very thin and much rough coating, resulting in a crisis at the substrate-coating interface already at low applied loads. The higher brittleness value is in agreement with the literature results regarding the deposition of thin films [62,63]:

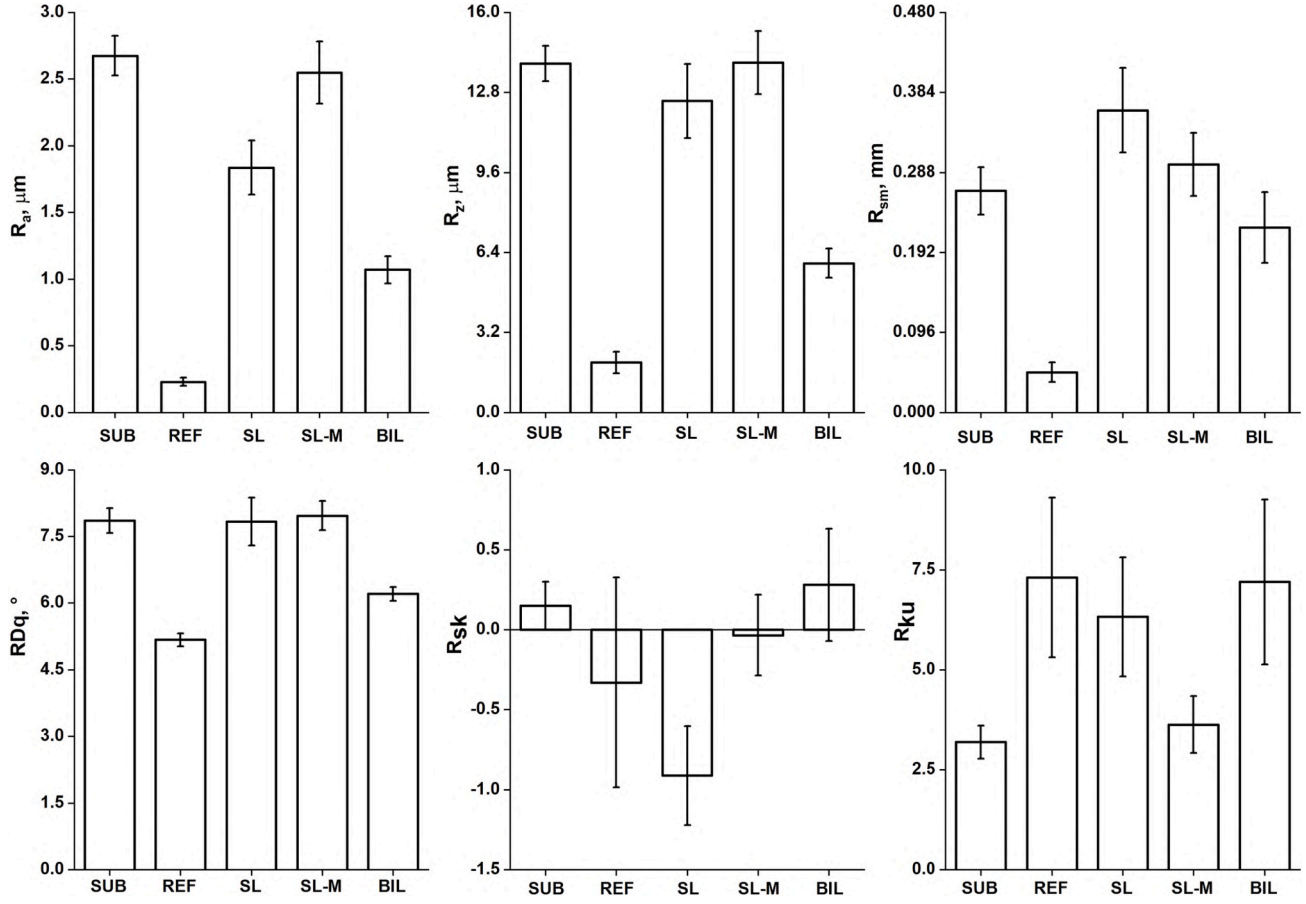

Fig. 17. Roughness analysis of yellow-coated samples. Please refer to Table A.2 in the Appendix for more details.

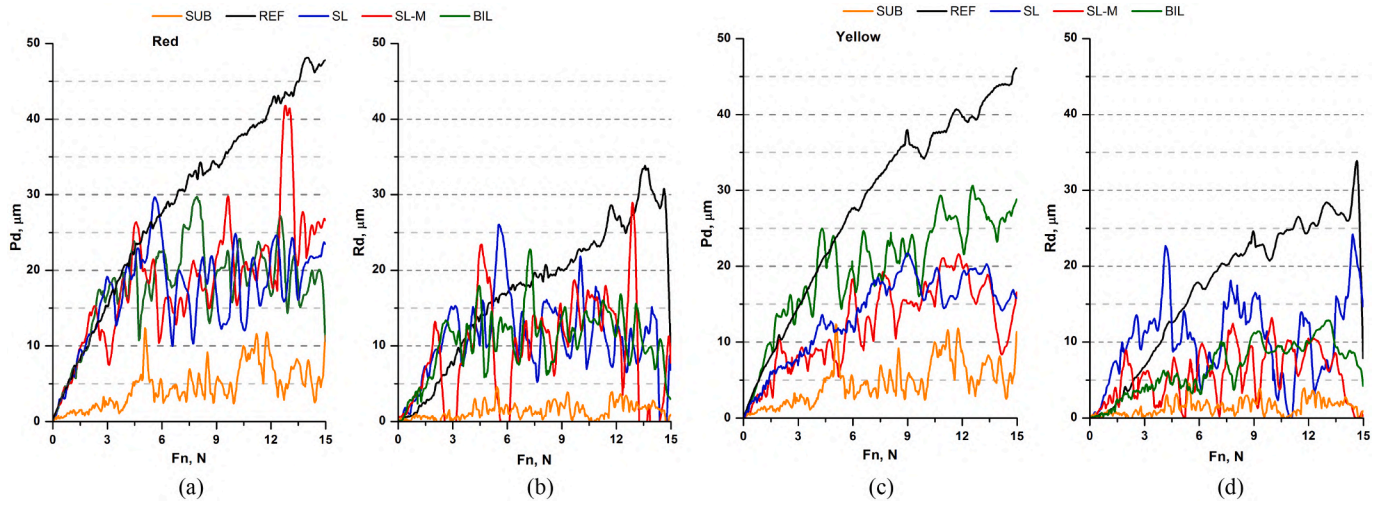

Fig. 18. Analysis of scratch test results: trend of penetration and residual depths as a function of normal force, measured per test on red (a–b) and yellow (c–d) coated samples. (For interpretation of the references to color in this figure legend, the reader is referred to the web version of this article.)

compared to a thicker coating, at the same normal load the stresses generated at the interface with the substrate are higher, thus with a tendency to failure and delamination of the coating. In SL-M specimens, there is a marginal reduction in the brittle behavior of the material, due to the addition of metal flakes, which strengthen the material, making it more elastic and resistant to deformation, according to [64,65]. In any case, this increase is quite small, as the results in Figs. 19 and 20 obviously consider also the deformation of the substrate, i.e. the special steel spring, which starts as early as at 3–5 N and continues until the end of the test, to which a large part of the overall deformation result is attributable. In fact, the very small values of R_d present in Fig. 18b–d for the SUB specimen underline its strongly elastic behavior, which is reflected in the results of Fig. 20.

Finally, BIL specimens present a slightly lower brittle deformation contribution than the SL ones, due to a greater coating thickness and similar P_d trends, as shown in Figs. 13 and 18a–c, conditions which

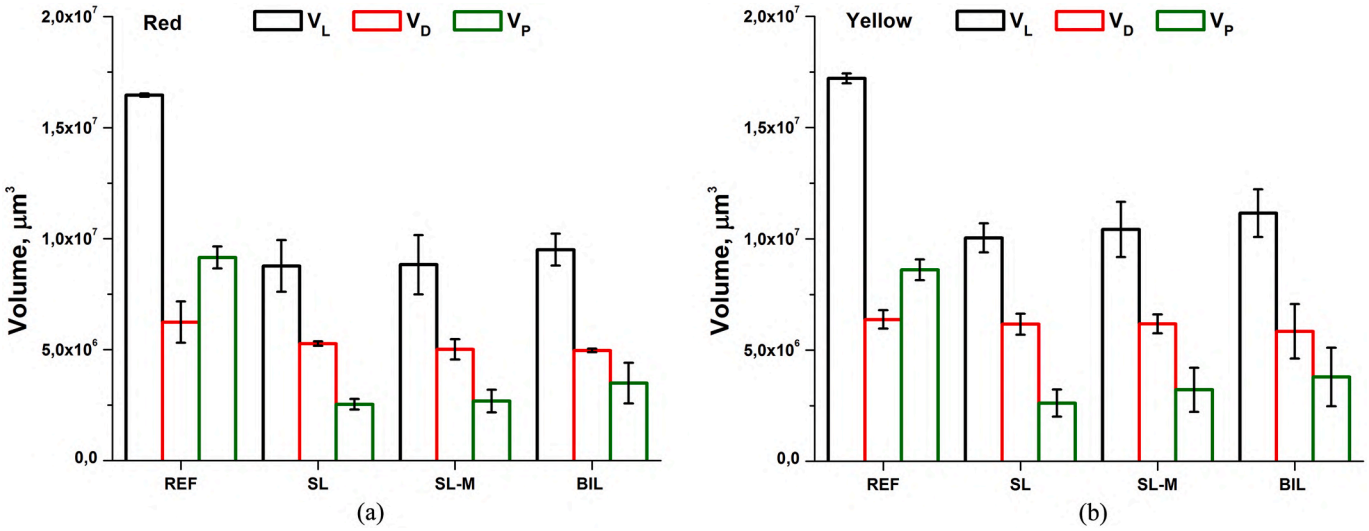

Fig. 19. Analysis of trace volumes under load (scan), of residual ditch and pile-up volumes (post-scan) for red (a) and yellow (b) coated samples. (For interpretation of the references to color in this figure legend, the reader is referred to the web version of this article.)

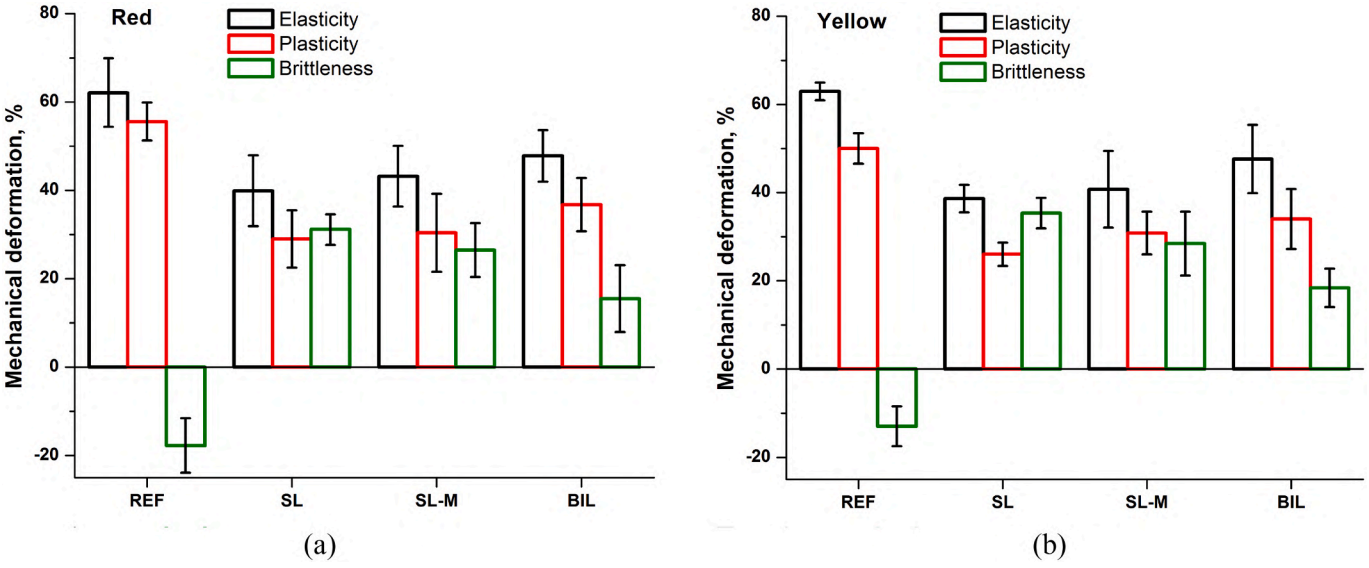

Fig. 20. Deformation contribution for red (a) and yellow (b) painted specimens. (For interpretation of the references to color in this figure legend, the reader is referred to the web version of this article.)

reduce the severity of the test at the coating-substrate interface. It follows that the lower stresses induced in the material allow its slightly higher share of elastic and plastic deformation. This is an important result, since BIL springs are covered by a greater coating thickness, so they are less affected by the springback of the substrate material, thus affecting the overall result less.

In summary, the results showed the validity of the solution of applying a bilayer, for the colors characterized by low coverage, namely red and yellow, allowing both to solve the problem of color uniformity, thus ensuring better protection of the substrate and improving the surface finish of the specimen, and to ensure a better mechanical behavior, due to a lower brittle deformation contribution.

4. Conclusions

This work dealt with an experimental study about the developing of an innovative FB-based powder deposition process for complex-geometry components. The case study presented dealt specifically with wire die springs, to be painted in different colors, as required by ISO 10243, depending on the severity of the cyclic load to resist. The need to study and develop an advanced coating system is related to the difficulty of deposition of a highly homogeneous, low-thickness coating, using traditional techniques, based on electrostatic systems, which tend to accumulate material in large quantities on the exposed surfaces, penetrating instead with difficulty into the recesses of the component, thus resulting in the need to deposit large quantities of powder to fully cover the component. This requirement is not only related to an aesthetic aspect, but also functional, since the polymer film acts as protection against the external environment and corrosive phenomena. Therefore, in order to avoid a waste of coating material and the deposition of a thick and non-uniform coating, with highly uneven mechanical and aesthetic characteristics, an innovative powder deposition system was proposed, whose most important results can be summarized as follows:

- The choice of adhesive primer and related solvent is decisive for the aesthetic and functional performance of the FB-based coating: applying a silicone primer diluted in a solvent with a high boiling point resulted in a coating with numerous holes that compromised its quality; choosing a solvent with a lower boiling point solved the problem, resulting in a coating much closer to the reference;
- The thickness of the innovative coating, i.e. ~15–20 μm, is significantly less compared to the traditional one, i.e. ~25–90 μm, with an excellent uniformity between the interior of the coils and the exterior surfaces, unlike the REF samples, which suffer from highly significant deviations; the deposition of a bilayer coating allows for increased thicknesses, providing greater coverage and uniformity;
- Color measurements on both the base and head of the springs, and on the inner coils, revealed how the FB-based deposition process is able to ensure excellent uniformity of coverage to all coils, unlike traditional ESD technology, which is characterized by considerable variability; the innovative technique ensures uniform coloration, with low deviation between the inside and outside of the sample, while the color difference between exposed and hidden areas between the coils is very pronounced in traditional ESD samples;
- For the blue and green colors, it was verified that SL process is optimal, depositing a coating with a uniform color and a homogeneous thickness of ~15–20 μm. In contrast, for the yellow and red colors, the addition of metal flakes to the coating improves the coverage of the substrate, but it causes excessive color variation from the REF. The application of a BIL solves this problem, proving to be an aesthetically optimal solution, especially for the yellow color;
- Due to the reduced thickness of polymer paint deposited, there is a memory effect for FB-based specimens, whose morphology is similar the SUB one. As a result, the roughness of the springs coated by the innovative system is greater than traditional one, i.e. R_a of ~2 μm and R_z of ~12–15 μm for the FB specimens versus values of R_a of ~0.3 μm and R_z of ~2.5 μm for the REF. The deposition of a BIL coating allows a more coverage of the initial roughness of the SUB, resulting in a coating with a better finish than the SL;
- The mechanical behavior of the wire die springs coated with the FB technique is not significantly affected by the presence of metal fillers; FB-based specimens are characterized by a scratch resistance similar to traditional ones for low loads, i.e. up to 3–5 N, while for higher loads, the penetration exceeds the coating thickness, verifying failure and delamination from the substrate, so a more brittle behavior, compared to REF. The application of a bilayer allows to improve the mechanical behavior, reducing the brittle contribution of the deformation.

In summary, it is possible to state that the innovative FB-based polymer powder deposition process has proven to be a viable alternative to traditional techniques, overcoming their main criticalities, allowing the deposition of coatings with low thickness and high uniformity even on complex-geometry components, also ensuring a significant reduction in powder consumption, as well as the possibility of coating even non-conductive components.

Funding

The authors declare that no funds, grants, or other support were received during the preparation of this manuscript.

CRediT authorship contribution statement

Gianluca Rubino: Conceptualization, Data curation, Formal analysis, Investigation, Methodology, Software, Resources, Supervision, Writing – review & editing. **Simone Venettacci:** Data curation, Formal analysis, Investigation, Software, Validation, Writing – original draft, Writing – review & editing.

Declaration of competing interest

The authors declare that they have no known competing financial interests or personal relationships that could have appeared to influence the work reported in this paper.

Appendix A

Table A.1
Roughness values of the red-coated samples.

Sample	R_a, μm	R_z, μm	R_{Sm}, mm	$R_{\Delta q}$, °	R_{sk}	R_{ku}
SUB	2.666 ± 0.221	14.124 ± 1.084	0.281 ± 0.031	7.952 ± 0.280	0.131 ± 0.224	3.375 ± 0.428
REF	0.352 ± 0.023	2.752 ± 0.405	0.076 ± 0.007	4.992 ± 0.177	0.013 ± 1.397	12.767 ± 19.888
SL	2.133 ± 0.230	14.816 ± 1.731	0.339 ± 0.044	9.164 ± 0.732	−1.428 ± 0.622	8.515 ± 3.085
SL-M	2.993 ± 0.371	16.467 ± 1.589	0.336 ± 0.035	8.650 ± 0.454	−0.376 ± 0.210	3.625 ± 0.518
BIL	2.202 ± 0.203	11.311 ± 0.850	0.400 ± 0.047	6.503 ± 0.153	−0.600 ± 0.203	5.315 ± 0.862

Table A.2
Roughness values of the yellow-coated samples.

Sample	R_a, μm	R_z, μm	R_{Sm}, mm	$R_{\Delta q}$, °	R_{sk}	R_{ku}
SUB	2.675 ± 0.149	13.952 ± 0.705	0.266 ± 0.028	7.857 ± 0.279	0,149 ± 0.151	3.190 ± 0.413
REF	0.229 ± 0.031	1.995 ± 0.434	0.048 ± 0.012	5.172 ± 0.144	−0.330 ± 3.560	22.401 ± 43.398
SL	1.836 ± 0.202	12.450 ± 1.482	0.363 ± 0.051	7.834 ± 0.540	−0.911 ± 0.309	6.322 ± 1.487
SL-M	2.548 ± 0.234	13.986 ± 1.263	0.297 ± 0.038	7.965 ± 0.330	−0.035 ± 0.252	3.625 ± 0.710
BIL	1.070 ± 0.101	5.965 ± 0.586	0.222 ± 0.043	6.204 ± 0.156	0.280 ± 0.651	5.292 ± 4.066

References

[1] Rodríguez-Barrero S, Fernández-Larrinoa J, Azkona I, de Lacalle LNL, Polvorosa R. Enhanced performance of nanostructured coatings for drilling by droplet elimination. Materials and Manufacturing Processes 2016;31:593–602. https://doi.org/10.1080/10426914.2014.973582.

[2] Lan P, Nunez EE, Polycarpou AA. Advanced polymeric coatings and their applications: green tribology. In: Hashmi S, Choudhury IA, editors. Encyclopedia of

renewable and sustainable materials. Oxford: Elsevier; 2020. p. 345–58. https://doi.org/10.1016/B978-0-12-803581-8.11466-3.
[3] Maiti TK, Parvate S, Pragya Singh J, Dixit P, Bhuvanesh E, et al. Plastics in coating applications. In: Hashmi MSJ, editor. Encyclopedia of materials: plastics and polymers. Oxford: Elsevier; 2022. p. 126–35. https://doi.org/10.1016/B978-0-12-820352-1.00176-0.
[4] Bahadori A. Chapter 2 - engineering and technical guidelines for painting. In: Bahadori A, editor. Essentials of coating, painting, and lining for the oil, gas and petrochemical industries. Boston: Gulf Professional Publishing; 2015. p. 107–56. https://doi.org/10.1016/B978-0-12-801407-3.00002-X.
[5] McKeen LW. 10 - application of liquid Coatings. In: McKeen LW, editor. Fluorinated coatings and finishes handbook. 2nd ed. Oxford: William Andrew Publishing; 2016. p. 171–83. https://doi.org/10.1016/B978-0-323-37126-1.00010-2.
[6] Richtering W. Polymer coatings: powder-based. In: KHJ Buschow, Cahn RW, Flemings MC, Ilschner B, Kramer EJ, Mahajan S, et al., editors. Encyclopedia of materials: science and technology. Oxford: Elsevier; 2001. p. 7233–4. https://doi.org/10.1016/B0-08-043152-6/01286–9.
[7] Crapper G. 10.29 - powder coatings. In: Matyjaszewski K, Möller M, editors. Polymer science: a comprehensive reference. Amsterdam: Elsevier; 2012. p. 541–66. https://doi.org/10.1016/B978-0-444-53349-4.00279-X.
[8] Manu- IF. Case study: conversion from liquid painting to powder coating. Metal Finishing 2013;111:35–6. https://doi.org/10.1016/S0026-0576(13)70283-6.
[9] van Dijken K, Prince Y, Wolters T, Frey M, Mussati G, Kalff P, et al. Industrial painting. In: Adoption of environmental innovations: the dynamics of innovation as interplay between business competence, environmental orientation and network involvement. Dordrecht: Springer Netherlands; 1999. p. 185–214. https://doi.org/10.1007/978-94-007-0854-9_12.
[10] Kotok V, Kovalenko V, Stathopoulos VN. Techniques for coating applications. In: Olabi A-G, editor. Encyclopedia of smart materials. Oxford: Elsevier; 2022. p. 243–57. https://doi.org/10.1016/B978-0-12-815732-9.00151-0.
[11] Albaladejo-Fuentes V, Maria Martos A, Silvello A, Dosta S, Sanchez J, Cano IG. Coatings, surface modifications, spray techniques (cold spray, HVOF/HVAF). In: Caballero FG, editor. Encyclopedia of materials: metals and alloys. Oxford: Elsevier; 2022. p. 451–64. https://doi.org/10.1016/B978-0-12-819726-4.00124-1.
[12] Hughes JF. Electrostatic powder coating. In: Meyers RA, editor. Encyclopedia of physical science and technology. 3rd ed. New York: Academic Press; 2003. p. 379–91. https://doi.org/10.1016/B0-12-227410-5/00219-2.
[13] Jaworek A, Sobczyk AT, Krupa A. Electrospray application to powder production and surface coating. J Aerosol Sci 2018;125:57–92. https://doi.org/10.1016/j.jaerosci.2018.04.006.
[14] Du Z, Wen S, Wang J, Yin C, Yu D, Luo J. The review of powder coatings. 2016. p. 54–9.
[15] Jozsef B, Blaga P. Factors that generate nonconformities in the electrostatic powder painting. Procedia Technology 2015;19:1089–93. https://doi.org/10.1016/j.protcy.2015.02.155.
[16] McKeen LW. 11 - powder coating and films. In: McKeen LW, editor. Fluorinated coatings and finishes handbook. 2nd ed. Oxford: William Andrew Publishing; 2016. p. 185–209. https://doi.org/10.1016/B978-0-323-37126-1.00011-4.
[17] Barletta M, Simone G, Tagliaferri V. A FEM model of conventional hot dipping coating process by using a fluidized bed. Prog Org Coat 2005;54:390–8. https://doi.org/10.1016/j.porgcoat.2005.09.004.
[18] Barletta M, Simone G, Tagliaferri V. Advance in fluidized bed coating: an experimental investigation on a performance polymer coating alloy. J Mater Process Technol 2006;178:170–80. https://doi.org/10.1016/j.jmatprotec.2006.03.171.
[19] Barletta M, Gisario A, Guarino S, Tagliaferri V. Fluidized bed coating of metal substrates by using high performance thermoplastic powders: statistical approach and neural network modelling. Eng Appl Artif Intel 2008;21:1130–43. https://doi.org/10.1016/j.engappai.2008.01.004.
[20] Leong KC, Lu GQ, Rudolph V. Comparative study of the fluidized-bed coating of cylindrical metal surfaces with various thermoplastic polymer powders. J Mater Process Technol 1999;89–90:354–60. https://doi.org/10.1016/S0924-0136(99)00045-X.
[21] Ayrilmis N. A review on electrostatic powder coatings for the furniture industry. Int J Adhes Adhes 2022;113:103062. https://doi.org/10.1016/j.ijadhadh.2021.103062.
[22] Bailey AG. The science and technology of electrostatic powder spraying, transport and coating. J Electrostat 1998;45:85–120. https://doi.org/10.1016/S0304-3886(98)00049-7.
[23] Barletta M, Tagliaferri V. Electrostatic fluidized bed deposition of a high performance polymeric powder on metallic substrates. Surf Coat Technol 2006;200:4282–90. https://doi.org/10.1016/j.surfcoat.2005.02.109.
[24] Osman H, Castle GSP, Adamiak K. Numerical study of particle deposition in electrostatic painting near a protrusion or indentation on a planar surface. J Electrostat 2015;77:58–68. https://doi.org/10.1016/j.elstat.2015.07.005.
[25] Rupp J, Guffey E, Jacobsen G. Electrostatic spray processes. Metal Finishing 2000;98:198–213. https://doi.org/10.1016/S0026-0576(00)80412-2.
[26] Barletta M, Gisario A, Guarino S, Rubino G. Development of smooth finishes in electrostatic fluidized bed (EFB) coating process of high-performance thermoplastic powders (PPA 571 H). Prog Org Coat 2006. https://doi.org/10.1016/j.porgcoat.2006.09.018.
[27] Barletta M. Electrostatic fluidized bed (EFB) coating of heat sensitive and electrical insulating substrates with low-curing thermoset epoxy-polyester (EP) powders. Prog Org Coat 2006;56:185–98. https://doi.org/10.1016/j.porgcoat.2006.04.002.
[28] Coatings P. Academic research in powder coating technology. Focus on Powder Coatings 2022;2022:1–2. https://doi.org/10.1016/j.fopow.2022.05.001.
[29] Biller K. New advances in powder coating technology. Coatings Tech 2021;18:18–23. https://doi.org/10.1016/j.fopow.2021.07.019.
[30] Whitehouse NR, Abdullahi AA. Inspection of paints and painting operations☆. In: Reference module in materials science and materials engineering. Elsevier; 2019. https://doi.org/10.1016/B978-0-12-803581-8.09830-1.
[31] Ye Q, Domnick J. On the simulation of space charge in electrostatic powder coating with a corona spray gun. Powder Technol 2003;135–136:250–60. https://doi.org/10.1016/j.powtec.2003.08.019.
[32] Emerging trends in powder coating technology. Focus on Powder Coatings 2020;2020:6. https://doi.org/10.1016/j.fopow.2020.01.028.
[33] Advancements in powder coating technology. Focus on Powder Coatings 2019;2019:1. https://doi.org/10.1016/j.fopow.2019.10.001.
[34] Misev TA, van der Linde R. Powder coatings technology: new developments at the turn of the century. Prog Org Coat 1997;34:160–8. https://doi.org/10.1016/S0300-9440(98)00029-0.
[35] Jis B. Wire die springs. 2012.
[36] Stampi MPER. ISO 10243 die springs. 2019.
[37] Springs D. ISO 10243. 2013.
[38] Coatings AP. Product data sheet. 2021. p. 7–9.
[39] Mazumder MK, Wankum DL, Sims RA, Mountain JR, Chen H, Pettit P, et al. Influence of powder properties on the performance of electrostatic coating process. J Electrostat 1997;40–41:369–74. https://doi.org/10.1016/S0304-3886(97)00073-9.
[40] Jaworek A, Sobczyk AT, Krupa A, Lackowski M, Czech T. Electrostatic deposition of nanothin films on metal substrate. Bulletin of the Polish Academy of Sciences: Technical Sciences 2009;57:63–70. https://doi.org/10.2478/v10175-010-0106-3.
[41] Barletta M. Progress in abrasive fluidized bed machining. J Mater Process Technol 2009;209:6087–102. https://doi.org/10.1016/j.jmatprotec.2009.04.009.
[42] Barletta M, Rubino G, Bolelli G, Lusvarghi L. Fast regime fluidized bed machining (FR-FBM) of thermally sprayed coatings. Journal of Thermal Spray Technology 2008. https://doi.org/10.1007/s11666-008-9266-1.
[43] el Hassanin A, Troiano M, Scherillo F, Silvestri AT, Contaldi V, Solimene R, et al. Rotation-assisted abrasive fluidised bed machining of alsi10mg parts made through selective laser melting technology. Procedia Manuf 2020;47:1043–9. https://doi.org/10.1016/j.promfg.2020.04.113.
[44] Venettacci S, Ponticelli GS, Guarino S. Fluidised bed finishing process for aeronautical applications: environmental and technical-economic assessment. J Clean Prod 2021;299:126900. https://doi.org/10.1016/j.jclepro.2021.126900.
[45] Barletta M, Guarino S, Vesco S, Gisario A, Tagliaferri V. Abrasive Fluidized Bed (AFB) finishing of thermally sprayed cobalt-chromium coatings. Manuf Lett 2013;1:1–4. https://doi.org/10.1016/j.mfglet.2013.08.002.
[46] Guarino S, Ponticelli GS, Tagliaferri F, Venettacci S. Life cycle analysis of an innovative fluidized bed degreasing process. J Clean Prod 2020;245:118947. https://doi.org/10.1016/j.jclepro.2019.118947.
[47] Coberth D, Ceyssons L. Stripping organic finishes with fluidized beds. Metal Finishing 2010;108:348–9. https://doi.org/10.1016/S0026-0576(10)80251-X.
[48] Barletta M, Gisario A, Venettacci S, Rubino G. A comparative evaluation of fluidized bed assisted drag finishing and centrifugal disk dry finishing. Engineering Science and Technology, an International Journal 2014;17:63–72. https://doi.org/10.1016/j.jestch.2014.03.007.
[49] Park SH, Kim SD. Oxygen plasma surface treatment of polymer powder in a fluidized bed reactor. Colloids Surf A Physicochem Eng Asp 1998;133:33–9. https://doi.org/10.1016/S0927-7757(97)00109-X.
[50] Bello MM, Abdul Raman AA, Purushothaman M. Applications of fluidized bed reactors in wastewater treatment – a review of the major design and operational parameters. J Clean Prod 2017;141:1492–514. https://doi.org/10.1016/j.jclepro.2016.09.148.
[51] Han Y, Wu C, Su Z, Fu X, Xu Y. Micro-electrolysis biological fluidized bed process for coking wastewater treatment. Journal of Water Process Engineering 2020;38:101624. https://doi.org/10.1016/j.jwpe.2020.101624.
[52] Barletta M, Trovalusci F, Gisario A, Venettacci S. New ways to the manufacturing of pigmented multi-layer protective coatings. Surf Coat Technol 2013:232. https://doi.org/10.1016/j.surfcoat.2013.06.113.
[53] Barletta M, Bolelli G, Guarino S, Lusvarghi L. Development of matte finishes in electrostatic (EFB) and conventional hot dipping (CHDFB) fluidized bed coating process. Prog Org Coat 2007;59:53–67. https://doi.org/10.1016/j.porgcoat.2007.01.012.
[54] de Almeida TH, de Almeida DH, Gonçalves D, Lahr FAR. Color variations in CIELAB coordinates for softwoods and hardwoods under the influence of artificial and natural weathering. Journal of Building Engineering 2021:35. https://doi.org/10.1016/j.jobe.2020.101965.
[55] Marinello F, Pezzuolo A. Application of ISO 25178 standard for multiscale 3D parametric assessment of surface topographies. IOP Conf Ser Earth Environ Sci 2019:275. https://doi.org/10.1088/1755-1315/275/1/012011.
[56] Barletta M, Tagliaferri V, Gisario A, Venettacci S. Progressive and constant load scratch testing of single- and multi-layered composite coatings. Tribol Int 2013:64. https://doi.org/10.1016/j.triboint.2013.03.002.
[57] Barletta M, Bolelli G, Gisario A, Lusvarghi L. Mechanical strength and wear resistance of protective coatings applied by fluidized bed (FB). Prog Org Coat 2008;61:262–82. https://doi.org/10.1016/j.porgcoat.2007.09.029.
[58] Barletta M, Gisario A, Rubino G, Lusvarghi L. Influence of scratch load and speed in scratch tests of bilayer powder coatings. Prog Org Coat 2009;64:247–58. https://doi.org/10.1016/j.porgcoat.2008.09.007.
[59] Gruda A. Overcoming outgassing issues during painting or powder coating of zinc-plated parts. Metal Finishing 2012;110:10–1. https://doi.org/10.1016/S0026-0576(13)70213-7.

[60] Barletta M, Tagliaferri V. Influence of process parameters in electrostatic fluidized bed coating. Surf Coat Technol 2006;200:4619–29. https://doi.org/10.1016/j.surfcoat.2005.04.030.
[61] Sanchez T, Zanna S, Seyeux A, Vaudescal M, Marcus P, Volovitch P, et al. Conversion coating distribution on rough substrates analyzed by combining surface analytical techniques. Appl Surf Sci 2021:556. https://doi.org/10.1016/j.apsusc.2021.149734.
[62] Favache A, Sacré CH, Coulombier M, Libralesso L, Guaino P, Raskin JP, et al. Fracture mechanics based analysis of the scratch resistance of thin brittle coatings on a soft interlayer. Wear 2015;330–331:461–8. https://doi.org/10.1016/j.wear.2015.01.081.
[63] Favache A, Daniel A, Teillet A, Pardoen T. Performance indices and selection of thin hard coatings on soft substrates for indentation and scratch resistance. Mater Des 2019;176:107827. https://doi.org/10.1016/j.matdes.2019.107827.
[64] Chavhan GR, Wankhade LN. Improvement of the mechanical properties of hybrid composites prepared by fibers, fiber-metals, and nano-filler particles-a review. Mater Today Proc 2020;27:72–82. https://doi.org/10.1016/j.matpr.2019.08.240.
[65] Gapsari F, Purnowidodo A, Setyarini PH, Suteja S, Abidin Z, Rangappa SM, et al. Flammability and mechanical properties of Timoho fiber-reinforced polyester composite combined with iron powder filler. J Mater Res Technol 2022;21:212–9. https://doi.org/10.1016/j.jmrt.2022.09.025.